Norwegian University of Life Sciences

Master's Thesis 2019 60 ECTS

Faculty of Chemistry, Biotechnology and Food Science

An investigation of wild-type P1 prophage induction

Ida Ormaasen

MSc Biotechnology

AN INVESTIGATION OF WILD-TYPE P1 PROPHAGE INDUCTION

Norwegian University of Life Sciences (NMBU),
Faculty of Chemistry, Biotechnology and Food Science

Acknowledgements

This thesis was performed at the Faculty of Chemistry, Biotechnology and Food Science, at Norwegian University of Life Sciences, under the supervision of Professor Knut Rudi.

First, I would like to thank my supervisor Knut Rudi. The door to your office was always open whenever I ran into challenges in the lab or had trouble with the writing. Your enthusiasm and positive attitude have inspired and encouraged me throughout the whole working process.

I would also like to thank Senior Engineer Morten Skaugen for performing the liquid chromatography-tandem mass spectrometry and the processing of the proteomics data. Thank you for all the help you have provided in relation to the laboratory work, data interpretation, and writing process.

Furthermore, I would like to thank Mari Hagbø and Laboratory Engineer Inga Leena Angell for all the guidance in the lab. Thanks to PhD Morten Nilsen for always being so helpful and supportive.

A big thanks to the master students Asima Locmic, Zuzanna Gulczyńska, Didrik Villard and Kasia Mielnicka for good company in the lab. This year would not have been the same without you.

Finally, thanks to friends and family who have encouraged and supported me throughout the whole year.

Ås, May 2019

Ida Ormaasen

Abstract

The spread of antibiotic resistance genes is increasing, and the mechanisms involved need to be established. Connections between the temperate bacteriophage P1 and antibiotic resistance genes have been implied. Therefore, the role phage P1 may possess in the dissemination of antibiotic resistance genes should be investigated. Since the mechanisms for transmission of wild-type bacteriophage P1 are poorly understood, this thesis aims to determine potential conditions that induce the lytic replication cycle.

Gene and protein expression of bacteriophage P1 were studied during different bacterial growth phases and temperatures. By quantitative PCR and bottom-up proteomics, the effects of exponential phase, stationary phase, 37°C and 42 °C were determined. In stationary phase at 42 °C, a significant increase in copy number of the *c*1 repressor gene was detected. The increase may imply derepression of *c*1. The difference in copy number of the lytic gene *pcp* was not significant, and no proteins were identified, indicating that no phage particle formation had occurred. A hypothetical protein with an ASCH resembling domain was significantly upregulated.

In addition, the study investigated how the conditions affected the Tn*21* transposon carried by P1. The copy number of the transposase gene *tnpA* was higher in stationary phase at the 42°C, compared to 37 °C, indicating that *tnpA* expression is temperature sensitive. Several antibiotic resistance proteins encoded by Tn*21* were identified. One of them was upregulated at both temperatures.

In conclusion, stationary phase physiology combined with elevated growth temperature may cause P1 prophage induction. However, in order to achieve lytic growth, additional inducing factors might need to be present. The Tn*21* transposon located in the P1 genome might have a higher transposition rate at elevated temperatures. Under the investigated conditions, P1 might contribute to the dissemination of antibiotic resistance genes by being a reservoir for transposons.

Sammendrag

Spredningen av antibiotikaresistensgener øker i omfang, og det er derfor et behov for å kartlegge mekanismene som er involvert. Forbindelser mellom den temperate bakteriofagen P1 og antibiotikaresistensgener har blitt antydet. Derfor burde bakteriofag P1 sin mulige rolle i spredningen av antibiotikaresistens undersøkes. Siden forståelsen av mekanismene for overføring av villtype bakteriofag P1 er mangelfull, er målet med denne oppgaven å bestemme mulige betingelser som kan indusere den lytiske replikasjonssyklusen.

Bakteriofag P1 sin gen- og proteinekspresjon ble studert under forskjellige bakterielle vekstfaser og temperaturer. Ved hjelp av kvantitativ PCR og proteomanalyse, ble effektene av eksponentiell fase, stasjonærfase, 37°C og 42 °C bestemt. I stasjonærfase ved 42 °C ble det detektert en signifikant økning i kopitall for *c*1 repressor genet. Økningen kan tyde på derepresjon av *c*1. Forskjellen i kopitall for det lytiske genet *pcp* var ikke signifikant, og ingen proteiner var identifisert, noe som tyder på at produksjon av viruspartikler ikke har funnet sted. Et hypotetisk protein med et domene som ligner ASCH-domenet var signifikant oppregulert.

I tillegg ble det undersøkt hvordan betingelsene påvirket Tn*21* transposonet i P1 bakteriofagen. Kopitallet til transposase-genet *tnpA* var høyere i stasjonærfase ved 42°C, sammenlignet med 37 °C, noe som indikerer at ekspresjonen av *tnpA* er temperatursensitiv. Tn*21* kodet for flere antibiotikaresistensproteiner som ble identifisert i analysen. En av dem var oppregulert ved begge temperaturer.

Den bakterielle fysiologien i stasjonærfase kombinert med forhøyet veksttemperatur kan trolig føre til induksjon av P1 profagen. Imidlertid, for å oppnå lytisk vekst, er det mulig at andre induserende faktorer må være tilstede. Tn*21* transposonet i P1 genomet har muligens en høyere transpososjonsrate ved forhøyede temperaturer. Under de undersøkte betingelsene er det mulig at P1 kan bidra til spredningen av antibiotikaresistensgener ved å være et reservoar for transposoner.

Abbreviations

AR	Antibiotic resistance
cDNA	complementary DNA
DNA	Deoxyribonucleic acid
ESBL	Extended spectrum beta lactamase
ESBL-E	ESBL-producing Enterobacteriaceae
FC	Fold change
HGT	Horizontal gene transfer
HRM	High resolution melting
LC-MS/MS	Liquid chromatography-tandem mass spectrometry
MGEs	Mobile genetic elements
mRNA	messenger RNA
m/z	Mass-to-charge ratio
NEC	Necrotizing enterocolitis
NICU	Neonatal intensive care unit
PCR	Polymerase chain reaction
RNA	Ribonucleic acid
rRNA	Ribosomal RNA
T16	Transconjugant 16
T30	Transconjugant 30

Table of Contents

1 INTRODUCTION

1.1 The human gut microbiota

A microbiota is the group of microorganisms in a specific habitat, and the microbiome is the collection of their genes (Turnbaugh *et al.*, 2007). The term microorganisms include all organisms, both prokaryotes and eukaryotes, that are too small to spot with the naked eye. Bacteria, viruses, fungi, archaea and protozoa are examples of microbes that are part of the human gut microbiota (Lozupone *et al.*, 2012; Morton *et al.*, 2015). The gut microbiota is considered to be an essential organ (Eckburg *et al.*, 2005). After many years of coevolution, it has gotten specialized to perform important tasks for the human body (McFall-Ngai *et al.*, 2013). In return, the microbes get a warm and nutritious place to live.

Trillions of microbes coexist in the human gut in a symbiotic, commensal or parasitic way. Their interactions with the host (human gut) can be indirect by impacting other microbes or direct (Kapitan *et al.*, 2018), and their influence affects the host digestion, immune maturation and protection against harmful microorganisms (Candela *et al.*, 2008; Fukuda *et al.*, 2011; Olszak *et al.*, 2012; Sonnenburg *et al.*, 2005). Compared to other microbial communities, the vertebrate gut microbiota encompasses great diversity (Ley *et al.*, 2008), and its capacity in the gut is just partly understood. The most studied part of the microbiota is the bacterial population, but to better understand the microbiota as a whole, research on the other constituents is done as well. The fungal fraction, known as the mycobiota, is involved in digestion and development of immune responses (Cuskin *et al.*, 2015; Zhang *et al.*, 2016). The gut viral population is the densest in the body, and consist of viruses targeting eukaryotes, archaea or bacteria. The gut virome comprises the collection of all viral genes in the intestine. Viruses using bacterial cells as hosts are called bacteriophages, and these make up the major part of the virome (Breitbart *et al.*, 2003). The virome is thought to be involved in immune system development as well as regulation of the gut bacterial population and bacterial evolution (Breitbart *et al.*, 2008; Takeuchi & Akira, 2009).

1.1.1 The gut mobilome

Collectively, the gut microbes harbor more genes than the human genome (Hamady & Knight, 2009). Some of these genes are located on sequences of DNA called mobile genetic elements (MGEs). MGEs can move around the genome or perform horizontal gene transfer (HGT) events (Partridge *et al.*, 2018). This moveable part of the microbiome and its genes is known as the mobilome. Exchange of genetic information in the microbiome allows traits to get spread among species, contributing to species evolvement (Broaders *et al.*, 2013; Huddleston, 2014). New traits can strengthen their fitness in the niches they are occupying.

1.1.2 The infant gut microbiota

Right after birth, the infant gut gets colonized by microbes. The following years the microbiota undergoes a myriad of compositional changes before an adult microbial composition is reached. The origin and type of microbes depend on delivery mode. Vaginally delivered babies get exposed to fecal and vaginal microbes from the mother while babies delivered by caesarean section get colonized by microbes derived from the mother's skin and the hospital environment (Backhed *et al.*, 2015).

While there is a global effort to elucidate the composition of the microbiota throughout life, there is a lack of knowledge on the recruitment of the gut virome. Nevertheless, several hypotheses have been suggested. The environment has been proposed to be a source (Lim *et al.*, 2015). Another hypothesis is that bacteriophages colonize the infant gut via their bacterial hosts (Breitbart *et al.*, 2008). Bacteriophages make up a substantial part of the infant virome and do also count as part of the mobilome. Considering that viruses and MGEs may affect the gut bacteria, and thereby the establishment and development of the microbiota, this should be looked more into. In fact, the infant gut has been proposed to be a reservoir for MGEs (Ravi *et al.*, 2015). A better understanding of the infant virome and mobilome is important in order to tackle the increasing problem of multidrug resistance in bacteria.

1.1.3 The preterm infant

One of the most vulnerable populations for microbial infections is the preterm infants. They are born before 37 weeks of pregnancy and are often experiencing serious health challenges (Ruiz *et al.*, 2016). Their organs and immune system may not be fully developed, and they are prone to develop necrotizing enterocolitis (NEC) and sepsis in which antibiotics is the only treatment (Milani *et al.*, 2017). Whether the preterm infant is colonized by pathogens carrying MGEs containing AR genes or not can be crucial for its survival throughout the first weeks of life (Ravi *et al.*, 2017). Again, this emphasizes the importance of a better understanding of the recruitment and characteristics of MGEs in the infant gut.

1.2 Antibiotic resistance

Antimicrobial resistance is an intrinsic defence mechanism in bacteria that occurs naturally in a competing environment as a response to bacteria with antimicrobial activity. Bacteria use two different strategies to adapt in an antimicrobial environment, 1) mutations in genes that often result in modification of an antimicrobial target, and 2) acquisition of anti-microbial resistance genes by horizontal gene transfer (Munita & Arias, 2016). This is seen in many different microbial communities, including the gut (Forsberg *et al.*, 2012; Rizzo *et al.*, 2013; von Wintersdorff *et al.*, 2014). The presence of various AR genes in the gut microbiome should therefore be no surprise, and the genes have even gotten their own term; the gut resistome (Penders *et al.*, 2013). Bacteria harbouring intrinsic antimicrobial resistance is not the main focus of the raising AR problem. The core of the problem is that pathogens acquire new AR traits, making it harder to combat bacterial infections (Munita & Arias, 2016).

Antibiotics have been produced and used to combat bacterial infections for almost 80 years. It has disarmed deadly bacterial pathogens and made cancer therapy, organ transplantations, complex surgeries and management of preterm infants possible by diminishing risk of complications caused by infection (Penders *et al.*, 2013). Overuse of antibiotics has increased the selective pressure towards multidrug resistance, and the development of new treatments does not meet the accelerating cases of infections caused by AR bacteria (Li & Webster, 2018). These infections pose a major cost for society due

to the need of prolonged hospital stays (OECD, 2018). As we are heading towards a post-antibiotic era where bacterial infections will be one of the leading causes of death, WHO has developed a global priority pathogens list to direct the research and development of new antibiotics into where it is most critically needed (Tacconelli *et al.*, 2018). Evaluation of 20 pathogens with 25 different resistance patterns was done based on several criteria. The criteria involved treatability and mortality, resistance trends and transmissibility, as well as burden and preventability in both the community and in the health-care system. The list was arranged into critical, high and medium priority. Out of the 20 evaluated bacteria, three bacterial species were characterized to be of critical priority, six of high priority and three of medium priority.

The three species of critical priority on the global priority pathogens list are antibiotic resistant Gram-negative bacteria. Two of them are the carbapenem-resistant Enterobacteriaceae and third-generation cephalosporin-resistant Enterobacteriaceae. Carbapenems are broad-spectrum antibiotics and often used as last-line agents, but with the emerging resistance in pathogenic bacteria, carbapenems life-saving capability is declining (Papp-Wallace *et al.*, 2011; Zilberberg *et al.*, 2017). The same applies for cephalosporins. Extended spectrum beta-lactamase (ESBL) is defined as an enzyme that can hydrolyse extended spectrum cephalosporin (Ghafourian *et al.*, 2015), thus disarming these drugs. Nosocomial and community-acquired infections caused by ESBL-producing Enterobacteriaceae (ESBL-E) are highly prevalent (Oli *et al.*, 2017; Park *et al.*, 2017; Pitout *et al.*, 2005). Enterobacteriaceae are common colonizers of the human gut (Lozupone *et al.*, 2012), but they are also associated with infections in the urinary tract (Karam *et al.*, 2019), gastrointestinal tract (Couturier *et al.*, 2011), lower respiratory tract (Dong *et al.*, 2018), central nervous system (Xu *et al.*, 2019), and blood system (Vihta *et al.*, 2018). Preterm infants are at risk to develop sepsis in the neonatal intensive care unit (NICU), and although infections caused by Gram-positive bacteria are most prevalent, the mortality of Gram-negative bacterial infections is higher (Shah *et al.*, 2015). There has been shown that mothers, without any previous symptoms of infections by ESBL-E, can transmit ESBL-E to their preterm babies, causing infection (O'Connor *et al.*, 2017). There has also been observed that ESBL-E can spread from one colonized preterm neonate to other neonates in the NICU by healthcare workers (Tschudin-Sutter *et al.*, 2010). These scenarios depict how easily antibiotic resistant bacteria can spread. Once the neonates are colonized, the ESBL genes can spread to other colonizers of the neonate gut (Brolund *et al.*, 2013). Luckily,

measures are being done to prevent dissemination, by performing ESBL-E screenings of expecting mothers and improving hygiene routines. Nevertheless, no new effective antibiotic class against Gram-negative bacteria has been approved in over 50 years, and as WHO stresses with the priority pathogens list, the need is critical. In addition, novel ways to tackle the dissemination of AR genes is essential.

1.3 Mobile genetic elements and horizontal gene transfer

MGEs include transposons, plasmids and bacteriophages (Naito & Pawlowska, 2016). They are DNA sequences that can move around the genome, be exchanged between bacteria or even between species. Transposons have intracellular mobility. Using their self-encoding transposase (TnpA), they can change position in a genome, or "jump" to other genetic elements in the same cell. The transposase makes a cut in the DNA sequence at the target site, producing sticky ends. Then it cuts out the transposon and ligates it into the target site (Levin & Moran, 2011). Transposon Tn*21* is a common MGE found in Enterobacteriaceae (Liebert *et al.,* 1999). It can carry integrons and gene cassettes with AR genes (Brown *et al.,* 1996). Integrons are non-mobile genetic elements that can integrate one or many gene cassettes. This is facilitated by its site-specific recombination system (Domingues *et al.,* 2012). Gene cassettes are DNA elements that often encode one single gene, and many do not have a promoter. As a part of an integron, the genes can be expressed by the promoter of the integron (Hall & Collis, 1995). Plasmids are self-replicating genetic elements found in bacterial cells. Typically, the plasmid is circular double stranded (ds) DNA, although linear plasmids with dsDNA also exist (Shintani *et al.,* 2015). IncI1 is a conjugal plasmid associated with carriage of ESBL (Carattoli, 2013).

HGT is the exchange of genetic information between bacteria (Burmeister, 2015). It is a form of homologous recombination, and occurs by transformation, conjugation or transduction. The mechanisms are illustrated in figure 1.1. Transformation is the process where cellular DNA is transferred between closely related bacteria (Johnston *et al.*, 2014). Both the transmitter cell and the receiver cell have genes in their genome that code for the transformation. Conjugation is the transmission of a conjugal plasmid among bacteria, and the whole process is encoded by the plasmid itself (Smillie *et al.*, 2010). DNA transfer

mediated by bacteriophages is called transduction (Olson, 2016). During packaging of the phage genome, sequences from the bacterial genome can get packed with it by mistake, thus resulting in transmission to a new bacterial cell. Transposons can get horizontally transferred by plasmids and bacteriophages if it has been translocated into these MGEs (Partridge *et al.*, 2018).

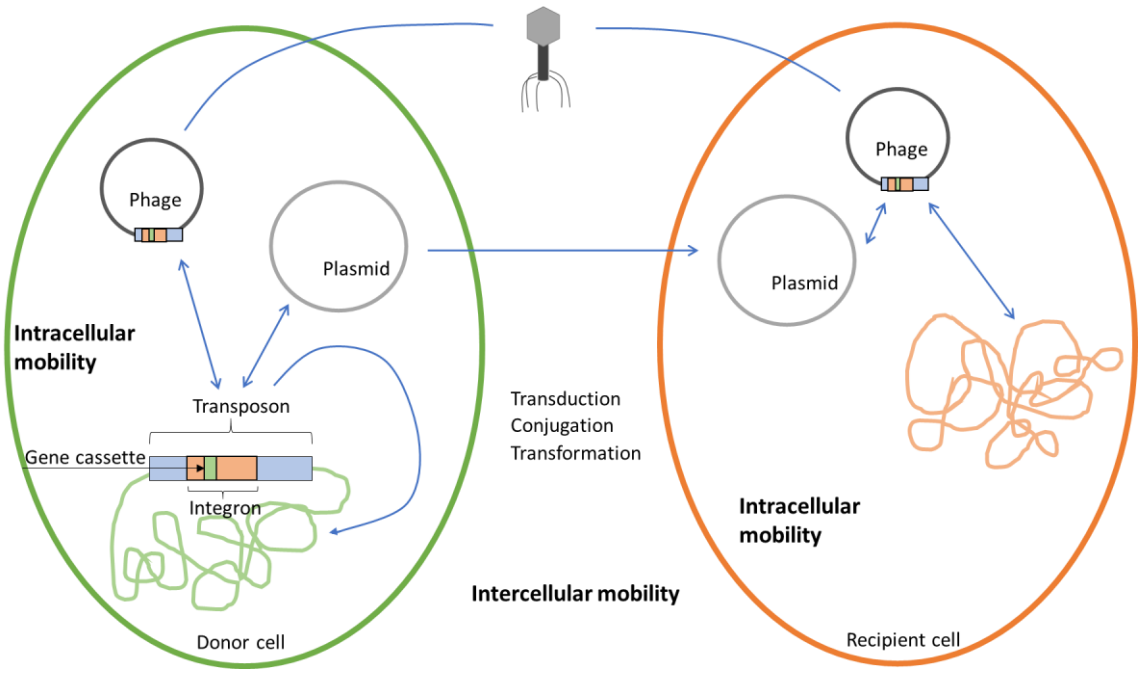

Figure 1.1: Mobile genetic elements and horizontal gene transfer. The figure gives an overview of MGEs and the different modes of MGE transmission. A gene cassette can be a part of an integron, which can be a part of a transposon. The transposon in the donor cell in the figure can translocate intracellularly between the phage genome, the plasmid, and different locations on the host genome. The phage and the plasmid are MGEs that have intercellular mobility. In the figure, the transposon gets transferred to the recipient cell by transduction, carried out by the phage. The plasmid transmits from the donor to the recipient cell by conjugation. In the recipient cell, the transposon can translocate to the host genome and the plasmid. Sequences of DNA can be exchanged between the donor and recipient cell by transformation (not illustrated). Transduction, conjugation and transformation are mechanisms of HGT. The figure is modified and redrawn from (Partridge *et al.*, 2018).

1.4 Bacteriophages

Since Twort and d'Herelle independently discovered the bacteriophage in the beginning of the last century, its abilities have been appreciated in a wide range of fields (Chan *et al.*, 2013; Ioannou *et al.*, 1994; Lennox, 1955). The bacteriophage, meaning something that devour bacteria, is a prokaryotic virus that hijack the replication machinery of its bacterial host in order to reproduce and make viral progeny.

The estimated number of bacteriophages in the biosphere is 10^{31} (Comeau *et al.*, 2008), making them the most numerous biological entity on the planet. Phages are the most abundant viral entity and they are believed to be found in every ecosystem (Sharma *et al.*, 2017). Because of their abundance and bacteria residing nature, they are significant influencers of bacterial populations and their environment.

1.4.1 Bacteriophage characteristics

There exists great diversity between phages when it comes to size, shape, complexity and genome composition. Their length varies from 24-200 nm. In comparison, the size of bacteria ranges from 0.2-2 μm. More than 6000 phages are described and a vast majority have a head-tail morphology, comprising an icosahedral capsid attached to a tail (Wittebole *et al.*, 2014). Three families in the *Caudovirales* order possess this morphology and their tail is either long and have a contractile sheath (*Myoviridae*), long and noncontractile (*Siphoviridae*) or short and noncontractile (*Podoviridae*). Bacteriophages can also have a filamentous, polyhedral or pleomorphic morphology (Ackermann & Prangishvili, 2012).

Phage genomes can be single stranded (ss) or double stranded RNA or DNA but are most commonly dsDNA (Hatfull & Hendrix, 2011). The genome sizes can range from 3.4 kilo bases (kb) to 500 kilo base pairs (kbp), and they are extensively mosaic (Casjens & Thuman-Commike, 2011; Hatfull & Hendrix, 2011). This means that the different segments of genes derive from different evolutionary histories. HGT is the reason for this complex genome structure.

1.4.2 Cell entry mechanism

The genomic material gets injected into the bacterial host cell after recognition and adsorption to the cell membrane. The latter is coordinated by the baseplate at the end of the tail and facilitated by the attached tail fibers. Phage tail fibers recognize specific receptors on the bacterial surface, and once all the fibers are bound to receptors, a conformational change in the subplate induces the genome injection. If the phage has a contractile sheath, the induction makes the sheath contract in a wavelike motion, exposing a tail tube that serves as a delivery channel for the genetic material (Leiman & Shneider, 2012).

1.4.3 Bacteriophage replication cycles

After genome delivery into the host cell, various scenarios can be played out depending on the type of phage. There exist four different replication cycles for bacteriophages. Filamentous phages can undergo a chronic replication cycle in which the phage replicates continuously and leaves the cell by a budding mechanism (Smeal *et al.*, 2017). In pseudolysogeny, the phage does neither propagate nor synchronize the replication of its genome with the host to maintain a stable copy number. This viral growth is often seen when access on nutrients is low (Cenens *et al.*, 2013). The two cycles best described are the lytic and lysogenic cycle, and these are elaborated in the following paragraphs and illustrated in figure 1.2.

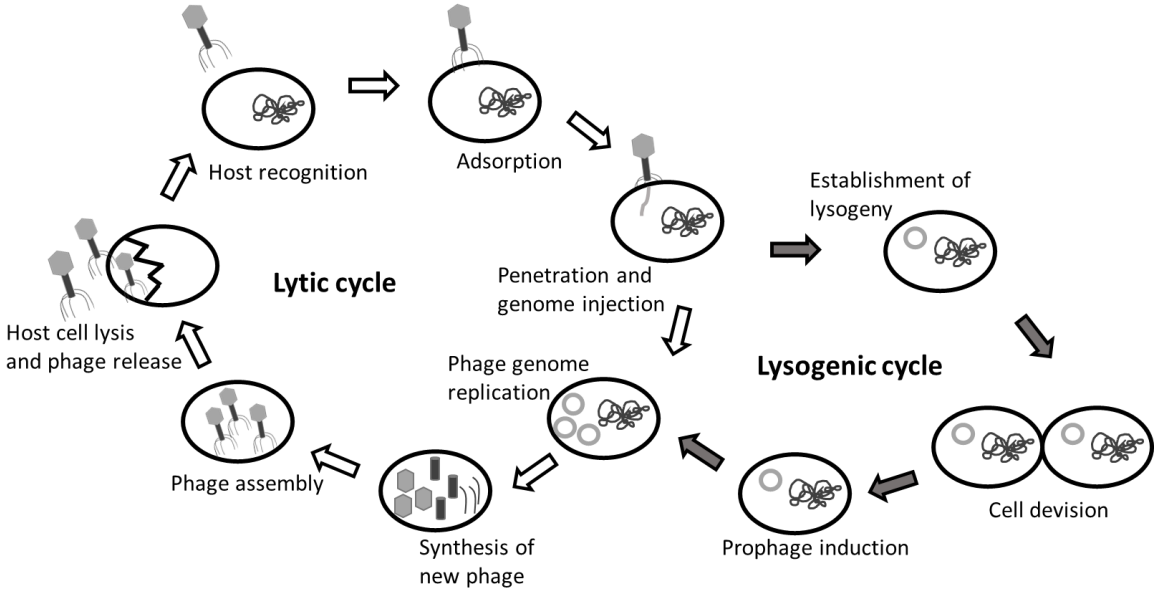

Figure 1.2: The lytic and lysogenic replication cycles of bacteriophages. The figure illustrates the lytic replication cycle, starting with recognition and adsorption to the host and injection of the genome into the host cytoplasm. Obligate lytic phages continue the lytic cycle proceeding with phage genome replication, while temperate phages, depending on external stimuli, may establish a lysogenic replication cycle. This illustration shows the prophage as a circular plasmid, but integration of the prophage into the host genome can also happen at this stage. The prophage replicates with the host. When external stimuli induce the prophage, it enters the lytic cycle and proceeds with lytic genome replication, phage particle production and lysis. Upon host cell lysis, phage particles are released and can infect new susceptible hosts. The figure is redrawn and modified from (Doss *et al.*, 2017).

1.4.3.1 Lytic replication cycle

The lytic replication cycle involves production of phages and cell lysis as the virus gets released and spread to new cells. The genomic material of the phage gets inserted into the host cell, and by use of the bacterial metabolic machinery, progeny virus is produced in great numbers (Sharma *et al.*, 2017). dsDNA genomes are directly transcribed to mRNA and translated to viral proteins, while ssDNA genomes are converted into dsDNA first. ssRNA genomes get synthesized to DNA by the viral enzyme reverse transcriptase before transcription (Choi, 2012). First, early genes involved in replication and transcription regulation are expressed. Then genes categorized as late genes like phage capsid protein and lysis protein encoding genes are expressed (Horcajadas *et al.*, 1999; Lavysh *et al.*, 2017). The nucleic acids are packed into synthesized capsids, before the cell bursts, letting phages infect new susceptible hosts.

1.4.3.2 Lysogenic replication cycle

Bacteriophages that can carry out a lysogenic cycle are called temperate phages and their bacterial hosts are called lysogens upon lysogenic growth. Temperate phages can integrate their genome into the host genome or be present in the cell as plasmids (Weinbauer, 2004). Whether the phage should lysogenize the host or enter the lytic life cycle right away is decided straight after infection. There are several factors affecting this decision. Pour physiological state of the host and low bacterial cell density are factors that favour lysogeny (Howard-Varona *et al.*, 2017). During lysogeny, the virus is called a prophage, and it is dormant. It replicates with the host and makes no harm to it (Weinbauer, 2004). The host becomes immune against infection of the same phage. The immunity is caused by a lytic repressor protein expressed by the prophage (Bondy-Denomy *et al.*, 2016). The functions involved in maintenance of lysogeny are therefore called the immunity system of the phage. External stress to the host, like UV radiation, chemicals or change in temperature cause prophage induction. Prophage induction involves several steps, leading to a lytic replication cycle (Choi *et al.*, 2010; Nanda *et al.*, 2014).

1.5 Bacteriophage P1

In 1951, microbial geneticist Giuseppe Bertani discovered bacteriophage P1, a phage that infects *Escherichia coli* and other enteric bacteria (Bertani, 1951). As it is a temperate phage, it lysogenizes its host cell and persists as a low-copy-number plasmid. Usually there is one plasmid per each bacterial chromosome, and it replicates independently of the host (Austin *et al.*, 1981). Belonging to the *Myoviridae* it has a typical head-tail morphology; an icosahedral head attached to a tail tube with a contractile sheath and baseplate with six tail fibers. Even though P1 has been utilized in the laboratory because of its transducing abilities for decades, playing an important role in the progression of molecular biology, little is understood of the underlying mechanisms of transduction (Pierce & Sternberg, 1992; Sternberg, 1990).

1.5.1 The P1 genome, replication and immunity

The P1 genome is approximately 93 kilo kbp dsDNA, and it contains approximately 117 genes divided into 45 operons (Lobocka *et al.*, 2004). An operon is a cluster of co-regulated genes that often have related functions (Osbourn & Field, 2009). In the P1 genome, four operons are crucial in the determination of lysogenic or lytic pathway, and four others are involved in plasmid maintenance. Most of the remaining operons are associated with lytic growth (Lobocka *et al.*, 2004).

1.5.1.1 Lysogenic replication and copy number control

The P1 replicon for lysogenic replication contains two operons and two regions of iterons. Iterons are repeated DNA sequences involved in plasmid copy number regulation (Chattoraj, 2000). One of the operons contains the gene that encodes replication protein A (RepA). RepA is an initiator protein involved in both replication initiation and control. It can bind to iterons in the origin region (*incC*) upstream for the *repA* gene and to iterons in the control region (*incA*) downstream for the *repA* gene. The *repA* promoter is situated in *incC*. The replicon is illustrated in figure 1.3 a. The operon involved in plasmid partitioning is located downstream of *incA* and it contains the two genes *parA* and *parB* (Lobocka *et al.*, 2004).

During lysogeny the prophage replicates to ensure inheritance in the cell line. Replication starts at the origin of replication (*oriR*), initiated by bound RepA, and proceeds in both directions on the genome. *incC* is a part of *oriR*. The plasmid partitioning protein A and B (ParA, ParB) are involved in the partition of the plasmid to host daughter cells (Lobocka *et al.*, 2004). P1 replication is strictly regulated by several mechanisms. One mechanism is the autoregulation of RepA synthesis. Replication is initiated when RepA reaches a threshold concentration. For this reason, suppression of the RepA concentration is necessary to repress replication (Lobocka *et al.*, 2004). This is attained as the iterons in *incA* sequester RepA.

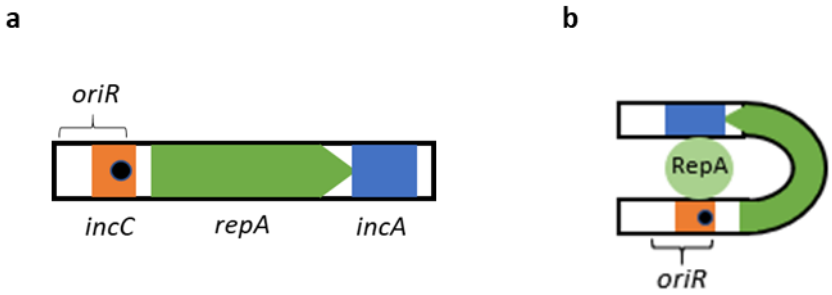

Figure 1.3: The lysogenic replicon. a) The replicon is depicted. The *repA* gene lies in between the upstream *incC* region and the *incA* region downstream of the gene. These regions contain iterons in which the RepA protein can bind. The *repA* promoter, indicated by a black circle, is situated among the iterons in *incC*. *oriR* precedes *repA*. **b)** illustrates the handcuffing mechanism. The iterons in *incA* are handcuffed to the iterons in *incC* by bound RepA. This leads to blocking of *oriR* and the *repA* promoter, resulting in inhibition of genome replication and *repA* transcription. The figure is adapted from (Pal *et al.*, 1986).

Since RepA is autoregulated, the natural consequence of sequestered RepA is replenishment of the protein. Phage P1 has a mechanism that avoids this by "handcuffing" the *incA* iterons to the iterons in *incC* via bound RepA. This pairing of iterons is illustrated in figure 1.3 b. The handcuffing cause sterical hindrance, blocking for both the replisome assembly and the *repA* promoter in *incA* (Chattoraj *et al.*, 1988). Consequently, the genome replication and *repA* transcription are inhibited.

1.5.1.2 Lytic replication of the P1 genome

The lytic replication of the genome is executed by the rolling circle mechanism (Cohen, 1983). This replication mechanism begins by forming a nick in one of the circular DNA strands. Then the nicked strand gets elongated by DNA polymerase at the 3' end using the unnicked strand as a template, resulting in a linear, ssDNA sequence. The linear strand is the lagging strand, and it is synthesized with a series of Okazaki fragments. This rolling circle replication results in a continuous linear DNA sequence of identical genomes, called a concatemer. The concatemer gets packed into the phage head until it is full (Coren *et al.*, 1995). The sequence is cut, a new head gets packed, and then the sequence is cut again. The head holds approximately 110 kbp DNA, and consequently a bit more than the genome gets packed (Sternberg *et al.*, 1990). Upon viral DNA delivery, the genome gets circularized into a plasmid in the host. Because of the DNA being cut out of a concatemer,

the phage genome is terminally redundant and cyclically permuted. The former meaning that the ends of the DNA molecule are identical, which enables DNA circularization, and the latter meaning that a given genome can start at any location on the circular genome.

1.5.1.3 P1 immunity

The immunity system of phage P1 encompasses the regions ImmC, ImmI and ImmT on the genome. The genes in these regions are involved in the decision-making between lytic and lysogenic establishment, and lysogenic maintenance (Heinrich *et al.*, 1994; Heinzel *et al.*, 1990; Heinzel *et al.*, 1992; Schaefer & Hays, 1990). The C1 protein is the key protein in lysogeny, repressing the lytic functions of P1 by binding to 17 different operators dispersed throughout the genome, in addition to regulate its own transcription (Lobocka *et al.*, 2004; Osborne *et al.*, 1989). An operator is the area upstream of an operon in which a repressor binds and repress transcription of the genes in the operon (Normanno *et al.*, 2012). The *c*1 gene is located in the ImmC region. Another gene within the ImmC region is the C1 antirepressor encoding *coi* gene (Heinzel *et al.*, 1990). *c*1 and *coi* belong to two different operators. Both operators are under the control of C1. The ImmI region contains an operon of three genes. *ant*1/2 encodes an antirepressor protein of C1. *icd* encodes an inhibitor of cell division and is required for *ant* expression. *c*4 encodes an antisense RNA that represses Icd and Ant1/2 synthesis. The ImmT region is located far away from the two other regions and contains the gene *lxc*. The Lxc protein is a corepressor of C1. It enhances operator binding of C1 by making a ternary operator-C1-Lxc complex. In addition, Lxc protects C1 against inhibition by Coi. In contrast to the two other regions, ImmT is not controlled by the C1 repressor. The connection between the repressors and their antirepressors is depicted in figure 1.4.

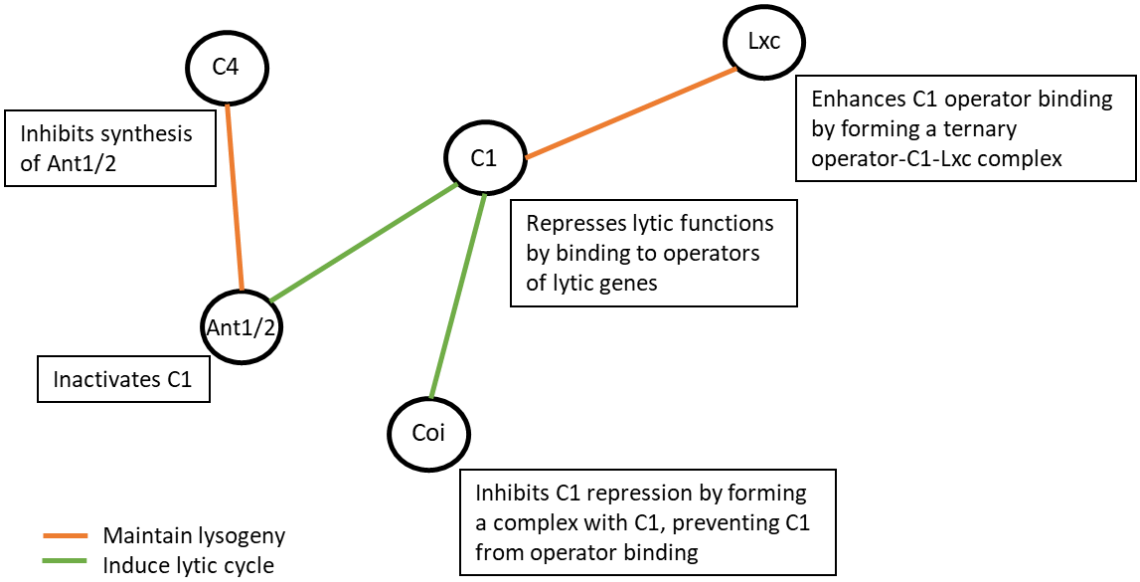

Figure 1.4: The P1 immunity system. The figure shows the connection between repressors and antirepressors of lytic growth. The C1 repressor, C4 antisense RNA secondary repressor, and Lxc corepressor maintain the lysogenic growth. C1 represses lytic growth. C4 and Lxc aid C1 by preventing C1 inactivation, and by enhancing the C1 effect, respectively. Ant1/2 and Coi induce lytic growth by inactivating C1. The illustration is made for this work. It is based on (Heinrich *et al.*, 1995).

When bacteriophage P1 infects a cell, it either enters the lytic cycle right away or chooses lysogeny. The transcription of *c*1 and *coi* is believed to happen simultaneously at this point and P1's lifecycle is determined by the protein that predominates. If that protein is Coi, C1 gets inactivated by becoming non-covalently bound to Coi (Heinzel *et al.*, 1990; Heinzel *et al.*, 1992). Consequently, operons regulated by C1 get expressed and lytic growth begins. If C1 synthesis prevails, C1 represses *coi* transcription by binding to its operator, initiating lysogeny (Heinzel *et al.*, 1990). When lysogeny is established, the C1 repressor, the secondary repressor C4 antisense RNA and the corepressor Lxc ensure maintenance of the lysogeny. (Citron & Schuster, 1990; Heinzel *et al.*, 1990; Schaefer & Hays, 1990).

1.6 Methods to measure gene expression

Gene expression is the conversion of genetic information into a functional protein (Segundo-Val & Sanz-Lozano, 2016). When a gene is activated, many mRNA containing the genetic information of the gene are made in a process called transcription. The mRNA is transferred from its production site in the nucleus to the cytoplasm, where it serves as a template for synthesis of the protein. The protein synthesis is called translation (Guo, 2014). The study of the transcripts of a cell can indirectly give an overview of the gene expression of a cell. Gene expression studies reveal gene functions and elaborate characteristics of organisms by studying the mRNA expression (Wang, Z. *et al.*, 2009). Due to the rapid degradation rate of mRNA, it is necessary in gene expression studies to convert mRNA into the more stable complementary DNA (cDNA).

1.6.1 Microarray

Microarray is a gene expression technique widely used for studying expression of many genes in a cell at the same time. The technique requires known genome information of the cell which is used to make DNA probes on a DNA chip. mRNA from the cell is extracted, converted to cDNA, fragmented and labelled with a fluorescent molecule. The microarray principle is based on hybridization of complementary sequences. When a cDNA fragment hybridizes to a complementary DNA probe, fluorescence is emitted and detected by a computer. Analysis of the emitted signals reveals all the genes expressed by the cell (Govindarajan *et al.*, 2012).

1.6.2 RNA sequencing

Another technique for studying the transcripts of a cell is RNA sequencing (RNA-Seq). Unlike microarray, RNA-Seq does not solely rely on genome annotation, and a sequencing platform is used to identify transcripts instead of a hybridization-based approach (Rao *et al.*, 2015). RNA from a cell is converted into cDNA, and all the fragments are gathered into one sample. The collection of all the fragments is called the cDNA library. The cDNA fragments get sequencing adapters on one or both ends, and the library is sequenced using high throughput sequencing like for instance Illumina IG (Morin *et al.*, 2008). The sequence information from the sequencing is aligned to a known genome or known

transcripts. It can also be assembled *de novo*, meaning putting together the sequence information without a reference genome (Wang, Z. *et al.*, 2009).

1.6.3 Real-time quantitative polymerase chain reaction

Real-time quantitative polymerase chain reaction (RT-qPCR or just qPCR) is yet another gene expression study approach. It is limited to studies done on a lower number of genes. RNA from the cells are extracted and converted to cDNA. The amount of cDNA for the genes of interest is analysed by qPCR using a dye that emits fluorescence when bound to dsDNA. The qPCR machine measures the fluorescence emitted in the end of each PCR cycle. The qPCR gives the results in Cq values which correspond to the number of cycles needed for the fluorescent signal to reach a predetermined threshold. The amount of each gene transcript, commonly referred to as the copy number, can be determined using a standard curve of the gene. By doing the same for a reference gene, the quantification can be normalized and used to observe gene expression under different conditions (Bustin *et al.*, 2005). The reference gene should be expressed equally in all the observed cells. The 16S rRNA gene is widely used as a reference gene in prokaryotes (Edwards & Saunders, 2001; Zhao *et al.*, 2019). However, it has been shown that expression of this gene varies depending on the conditions the prokaryotes are put under (Vandecasteele *et al.*, 2001). Hence, it does not serve as an ideal reference gene.

1.7 Proteome analysis

A proteome is the total amount of proteins expressed by an organism (Encarnacion-Guevara, 2017). The proteome can be analysed using advanced technology, identifying the proteins expressed at a given time and their abundance. While genomics and transcriptomics show the potential of an organism, proteomics unveil the actual functions.

Liquid chromatography-tandem mass spectrometry (LC-MS/MS) is widely used in proteome analysis for identification of proteins (Karpievitch *et al.*, 2010). The method separates the compounds in the sample by liquid chromatography. Further, the mass-to-charge ratios (m/z) of the compounds are detected and used for identification. The

compound detection results in a mass spectrum where the m/z and abundance of the compound is illustrated as a peak. The most abundant compounds are chosen for a MS/MS analysis where they are fragmented, resulting in smaller constituents with their own m/z, and measured by the detector. Several fragmentation events increase the sensitivity of the proteome analysis.

Bottom-up proteomics is a method used in the protein characterization of a proteome (Zhang *et al.*, 2013. In this method the isolated proteins are proteolyzed into peptides, and the characterization is achieved by analysis of these peptides, typically by LC-MS/MS. The raw data from the analysis are processed and used to search a protein database. Matches to the database are based on the accurate mass of the intact peptide (precursor mass) and on the fragments generated in MS/MS (sequence data). Further processing is necessary to remove false hits and potential contaminants. The number of peptides matched to a protein and the number of unique peptides matched to the protein indicate the confidence of the protein identification. Unique peptides are peptides that only match to one protein. The protein identification is strengthened by many matched peptides and in which many of them are unique. Additionally, the sequence coverage can be evaluated, indicating how much of the protein sequence that is covered by the matched peptides. Statistical analysis like t-tests and volcano plots are done to evaluate proteomics results, and heatmaps are used for visualization (Oveland *et al.*, 2015). To identify proteins with high fold changes in expression and high statistical significance, Volcano plots are used to identify proteins with high fold changes in expression and high statistical significance. A heatmap show the expression levels of proteins. By using colour intensity, heatmaps visualize down- and upregulation.

1.8 Aim of thesis

This thesis is a continuation of research executed by Mari Hagbø as part of her master thesis (Hagbø, 2017). The research involved a conjugation experiment where the wild-type bacteriophage P1 got transferred from a clinical isolate to the recipient strain. To our knowledge, wild-type P1 transmission has not been observed before. The mechanisms for transmission are poorly understood, and as associations between P1 and AR genes have been drawn (Billard-Pomares *et al.*, 2014; Yang *et al.*, 2017), the transmission of the bacteriophage should be investigated more thoroughly.

Therefore, the aim of this thesis was to better understand bacteriophage P1 transmission by determining potential conditions that induce the lytic replication cycle. To investigate this, several sub goals were included.

- Characterize the growth and cultures of the P1 transconjugants and the recipient strain *E. coli* DH5α-Rif^{R}.
- Explore effects of growth phase and temperature on gene expression of specific P1 genes involved in repression of the lytic cycle, genome replication, structure of the phage particle, and a Tn*21* transposition gene.
- Explore effects of growth phase and temperature on the P1 proteome.
- Create a model for the early phase of prophage induction.

2 MATERIALS AND METHODS

A schematic overview of the experiments is given in figure 2.1.

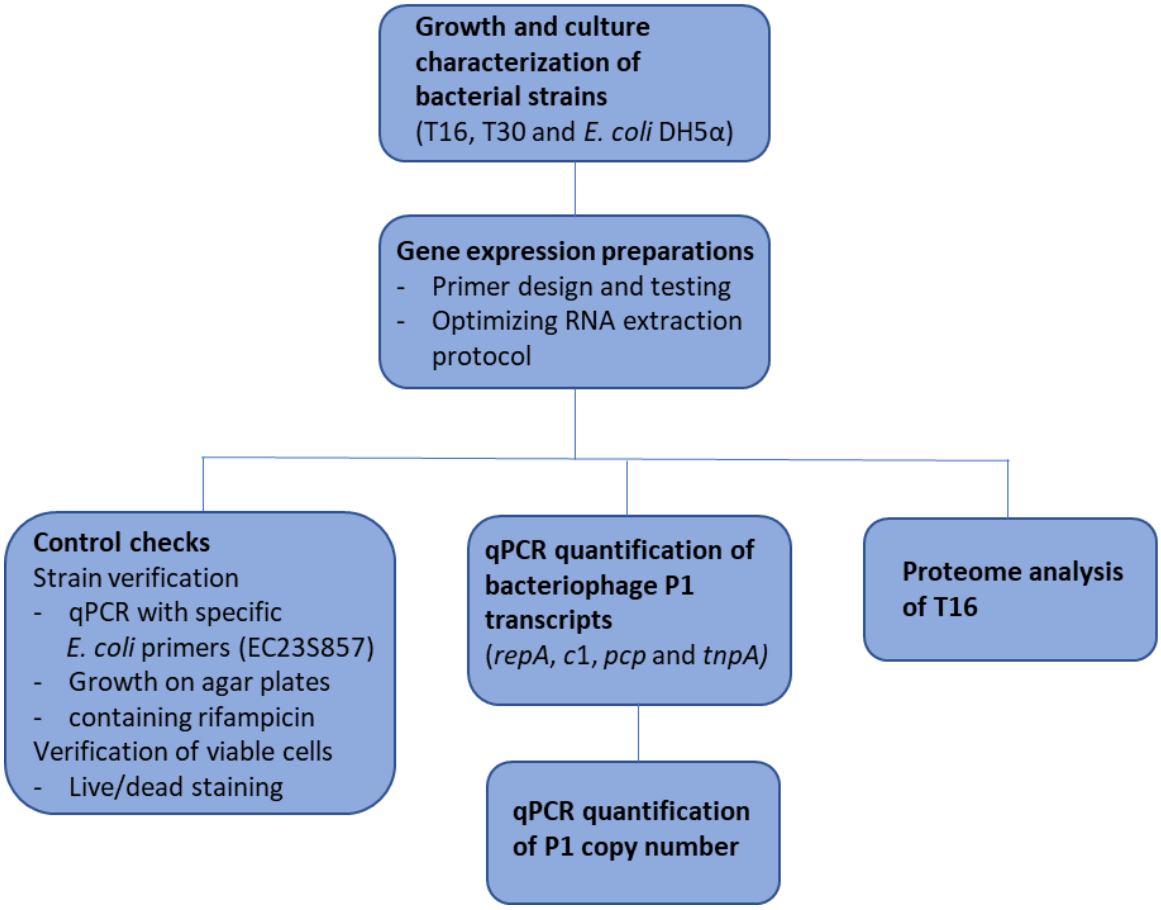

Figure 2.1: Flow chart of the experimental set up. The figure gives an overview of the experiments.

2.1 Background information and overview of bacterial strains

The donor strain in the conjugation experiment performed by Mari Hagbø was *E. coli* isolated from a fecal sample of a Spanish preterm infant (Hagbø, 2017). The gestational age of the infant was 30 weeks, and it had been delivered by emergency caesarean section. The infant was breastfed and had not been treated with antibiotics prior to the sample collection. The collection had taken place 20 days after delivery. Several mobile genetic elements were found in bacterial isolates in addition to the P1 phage, including the conjugal

plasmid IncI1 and the transposon Tn*21*. During the conjugation experiment, incidences of Tn*21* translocation to bacteriophage P1 had occurred.

In this work, the experiments were performed on two transconjugants and the laboratory strain *E. coli* DH5α - Rif^R as a control. *E. coli* DH5α - Rif^R is a mutant of resistant to 320 µl/ml rifampicin. The transconjugants were MGE containing *E. coli* DH5α - Rif^R and derived from the mentioned conjugation experiment. Transconjugant 16 (T16) contained bacteriophage P1, and transconjugant 30 (T30) contained both bacteriophage P1 and the IncI1 plasmid. The P1 phage in this experiment carried the Tn*21* transposon.

2.2 Growth conditions

Growth media used in the experiments were Müller Hinton (MH) agar (Oxoid Ltd, UK) containing 320 µl/ml rifampicin (Sigma-Aldrich, Norway AS), Luria-Bertani (LB) agar and LB broth. See appendix A for the reagents used in LB agar and broth.

Bacterial cells from glycerol stocks were spread on LB agar plates and incubated at 37 °C over night. LB broth was inoculated with one colony isolated from an agar plate and incubated at 37 °C or 42 °C, and 120 rpm.

For colony counts, 10-fold dilutions of the bacterial culture were made, and 100 µl was spread on LB agar plates. The agar plates were incubated at 37 °C over night.

Optical density (OD_{600}) of the strain cultures was measured in a McFarland densitometer (BioSan, EU). The method measures the time that light uses to pass through a liquid solution. The more cells there are in a culture, the more time the light uses.
Exponential phase was reached when the cultures had an OD_{600} around 0.5. This was measured in a McFarland densitometer (BioSan, EU). Stationary phase was reached over night.

2.3 Polymerase chain reactions

Detailed information about the primers used in the PCR reactions is given in table 2.1

2.3.1 Primer design

Primers for several genes of interest were designed using Geneious (version 10). The primer design based on sequencing data of bacteriophage P1- and IncI1-containing transconjugants produced by Mari Hagbø. The desirable characteristics of the primers were a GC-content between 50-60%, a melting temperature between 55-65 °C and a G or C located at the end of the primer sequence. The sequence length of the amplicon should be about 150 bp. These characteristics were plotted into the Geneious primer design function, and the primers that best matched the qualifications were selected and designed to be used in the experiments.

2.3.2 Qualitative PCR

The reaction mix consisted of 1x HOT FIREPol® (Solis BioDyne, Estonia), 0.2 µM of each primer, nuclease-free water and 1 µl DNA template. It all added up to a final volume of 25 µl per reaction. Amplification was performed on 2720 Thermal Cycler (Applied Biosystems, USA) using the following program: 15 min of initial denaturation at 95 °C followed by 25 cycles of denaturation at 95 °C for 30 sec, annealing at 60 °C for 30 sec and elongation at 72 °C for 30 sec before final elongation at 72 °C for 7 min.
Gradient PCR was performed to determine optimal annealing temperatures of the primers. This was accomplished using the reaction mix and program mentioned above on a Mastercycler® gradient (Eppendorf, Germany). The temperature gradient was set at ± 7 °C, resulting in annealing temperatures spanning from 53-67 °C. The PCR products were analysed with gel electrophoresis.

2.3.3 Quantitative PCR

The reaction mix contained 1x Hot FIREPol® EvaGreen qPCR supermix (Solis BioDyne, Estonia), 0.2 µl of each primer, nuclease-free water and 1 µl DNA template. The final volume was 20 µl per reaction. The amplification was performed with the following

program on the CFX96 Touch™ Real-Time PCR Detection System (Bio-Rad, USA): Initial denaturation at 95 °C followed by 40 cycles of denaturation at 95 °C for 30 sec, annealing at 60 °C for 30 sec and elongation at 72 °C for 45 sec.

Table 2.1: **Primers used in PCR.** There are two different sets of primers for each of the P1 genes (*repA, c*1, *pcp* and *repA*); primer pair 1 and primer pair 2.

Target gene	Primer	Amplicon length (bp)	Primer sequences F/R (5' – 3')	Reference
repA	repA_1_F repA_1_R	150	TCGCGGATCGTCAGTTACAA/ GTTATGCCCACCCACACCTT	This work
	repA_2_F repA_2_R	150	CTCCGCGTTGTTTGACTACG/ GTCTGCTGAATGCGTGTCAG	
***c*1**	c1_1_F c1_1_R	150	AGTGCCTAACATCCTTCGCG/ GCACTGTGCTCATTGATCCC	This work
	c1_2_F c1_2_R	200	TGTCTACGGCGAACAACTGT/ TTCCAGTTCTCGCGCCATTA	
***pcp* (phage capsid protein)**	pcp_1_F pcp_1_R	150	ATCGAAAATTCCCGGCCAGA/ TCGCGTAGTTGATTTGGCCT	This work
	pcp_2_F pcp_2_R	150	AGGCCAAATCAACTACGCGA/ CATCGCGTTGGTTTTGGCTT	
tnpA	tnpA_1_F tnpA_1_R	150	GCCCAGGACGGACTTTCTAC/ CGGTGTAGTGCTCCTCGATC	This work
	tnpA_2_F tnpA_2_R	150	ATCACGTCTTCGCCCTGATG/ CGTGCTTGATGTTGAGCGTG	
16S rRNA (V3 and V4 region)	PRK341 F PRK806 R	466	TCCTACGGGAGGCAGCAGT/ GGACTACCAGGGTATCTAATCCTGT	(Nadkarni *et al.*, 2002)
23S rRNA (*E. coli*)	EC23S857 F EC23S857 R	88	GGTAGAGCACTGTTTtGGCA/ TGTCTCCCGTGATAACtTTCTC	(Chern *et al.*, 2011)

2.3.4 **Purification of PCR product**

PCR products were purified by size selective precipitation. Ampure XP beads (Beckman Coulter, USA) with a final concentration of 1.5x was used in order to extract DNA fragments of the size of the amplicons. The ampure XP beads are paramagnetic and have affinity for DNA. Using a magnet, the beads with the DNA were pelleted and the supernatant was removed and discarded. The beads were washed two times with 80 %

ethanol before DNA elution was achieved using nuclease-free water as elution buffer. The same volume as the sample volume was used.

2.4 Gene expression

2.4.1 Sample preparation

Cultures of the transconjugants and E. coli DH5α - Rif^R were grown, and samples of 1 ml and 500 µl were taken during exponential growth phase and stationary growth, respectively. The samples were pelleted and washed with 1x Phosphore Buffered Saline (PBS) corresponding to the initial volume. See appendix A for PBS reagents. The cells were dissolved in a small volume of 1x PBS, and RNALater (Invitrogen, USA) was added in a 1:5 ratio for RNA stabalization. The cell suspensions were stored at -20 °C.

2.4.2 RNA extraction

RNA was extracted from the cell suspensions both manually and automatically with KingFisher Flex robot (Thermo Scientific, USA) using the MagMax™-96 Total RNA isolation kit (ThermoFisher Scientific, USA). The kit employs a guanidinium thioacetate-based lysis buffer that dissolves the cell membranes and inactivates nucleases. Paramagnetic beads with affinity for RNA removed the RNA from the suspension in the presence of a magnet, and contaminants were washed away. The nucleic acids were treated with DNase to remove DNA. A low concentrated salt buffer eluted the RNA from the beads.

2.4.3 Additional DNase step

To remove excess DNA in the RNA eluates, an additional DNase step was performed manually using the TURBO DNA-free™ Kit (ThermoFisher Scientific, USA). TURBO DNase is more efficient compared to the DNase used in the MagMax™-96 Total RNA isolation kit and ensures considerably improved DNA contamination removal. The treatment was performed in correspondence with the manufacturer's recommendations, following the routine DNase treatment (≤200g µg nucleic acid per ml).

2.4.4 cDNA synthesis

cDNA synthesis was performed on the DNase treated RNA eluates using the FIREScript RT cDNA Synthesis Mix (Solis BioDyne, Estonia). The reaction solution consisted of 1x RT Reaction Premix with Random Primers, 1.5 µl FIREScript Enzyme Mix, approximately 65 ng template RNA and nuclease free water. The final volume was 20 µl. The synthesis was executed using the following program: Primer annealing at 25 °C for 5 min, reverse transcription at 50 °C for 30 min and enzyme inactivation at 85 °C for 5 min.

2.5 DNA and RNA quantification and qualification

2.5.1 Qubit quantification

DNA and RNA were quantified using Qubit® dsDNA HS Assay Kit and Qubit® RNA HS Assay Kit (Invitrogen, USA), respectively. The former assay includes a dye highly selective for dsDNA, and the latter uses a dye highly selective for RNA. The dye, when bound to the nucleic acids, emits fluorescence which can be detected in a Qubit Fluorometer (Invitrogen, USA). The assays were executed according to the manufacturer's recommendations using 2 µl sample and 198 µl working solution.

2.5.2 Gel electrophoresis

Qualification of nucleic acid fragments was achieved by gel electrophoresis in 1.5 % agarose gel consisting of agarose (Invitrogen, USA) and 1x tris-acetate EDTA (TAE) buffer. The agarose molecules in the gel create a network, and when electrical voltage makes the negatively charged fragments migrate through the gel, they get separated by size. Voltage, ampere and time were set to 80 V, 400 amp and 30 min, respectively. The bands were stained with the dye PeqGreen (Peqlab, Germany) which binds to nucleic acids and emits fluorescence when bound. The bands were visualized by UV light using the MolecularImager® Gel Doc™ XR Imaging system with Quantity One 1-D analysis software (v. 4.6.7) (BioRad, USA). As reference, a 100 bp ladder (Solis BioDyne, Estonia) was used.

2.5.3 High resolution melting analysis

High resolution melting (HRM) analysis make use of the fact that different amplicons contain different amounts of the bases G and C. The GC-content determines the melting point of an amplicon, and in this way, amplicons can be identified. The method is used to verify the presence of desired amplicons after qPCR analyses. At the end of each run, a HRM analysis was performed by rising the temperature from 60 °C to 95 °C in the CFX96 Touch™ Real-Time PCR Detection System (Bio-Rad, USA)., and the melting temperatures of the amplicons were detected.

2.6 Microscopy

Two microscopy methods were performed. Light microscopy is a quick method to observe cell morphologies present in a culture. Fluorescence microscopy of stained bacterial cells visualize the viability of bacterial cells. LIVE/DEAD BacLight Bacterial Viability Kit (LIVE/DEAD stain, Invitrogen™, Molecular Probes Inc., USA) include two nucleic acid binding fluorescent dyes that can help distinguish between viable and non-viable cells. The dye SYTO9 stains cells with an intact cell membrane and they appear fluorescent green in the microscope. Propidium iodide stains cells without or partly without a cell membrane and they appear fluorescent red. Dying cells appear yellow. The procedure was performed after the manufacturer's recommendations.

2.7 Proteome analysis

The LC-MS/MS analysis and processing of proteomics data were performed by Senior Engineer Morten Skaugen.

2.7.1 Protein extraction

The bacterial cells were grown in LB broth at 37 °C and 42 °C, and sampled in the stationary growth phase. The samples were pelleted and resuspended in 500 µl 4 % SDS,

50 mM Tris and 10 mM dithiothreitol (DTT). The proteins solubilized in the solution after lysing of the cells using a combination of heating and shaking with acid washed glass beads (106 µm) using FastPrep96 (MP Biomedicals, France). The samples were centrifuged. The supernatants were retained and stored at -20 °C awaiting further processing.

2.7.2 **Peptide isolation**

The method used for peptide isolation is based on Zougman, Selby and Banks suspension trapping sample preparation method (Zougman *et al.*, 2014). A column for each sample was made using two types of filters, a quartz filter on top of a C18 filter, and installed in a collection tube. This made up the centrifuge assembly. The column was filled with suspension trapping (STrap) solution (90 % methanol, 100 mM Tris pH 7.1). The protein sample was incubated at 47 °C to dissolve the SDS in the sample. Iodoacetamide (IAA) (Sigma-Aldrich, Norway AS) was added to the samples to a final concentration of 50 mM before incubation in the dark for 20 min. The sample was acidified by phosphoric acid (PA) (Sigma-Aldrich, Norway AS), resulting in a final PA concentration of 1.2 %, and added in the top third of the STrap solution in the column. Due to the acidic sample and the neutral methanol in the STrap solution, the proteins precipitated. Upon centrifugation, the proteins got trapped in the quartz filter, while contaminants, together with the SDS, flowed through. The column was first washed with STrap solution to remove SDS remnants, then with 50 mM ammonium bicarbonate $(NH_4)HCO_3$) (Sigma-Aldrich, Norway AS) to make the column alkaline before trypsin digestion. The proteins were incubated with trypsin (33 ng/µl in 50 mM $(NH_4)HCO_3$) at 47 °C for 1 h. After incubation, the assembly was centrifuged briefly. The flow through was mixed with trifluoroacetic acid (TFA) solution 1 (0.5 % in H_2O) (Sigma-Aldrich, Norway AS) and added to the column before re-centrifugation. At this point, the peptides had gone through the quartz filter and gotten trapped in the C18 filter. The column was washed by TFA solution 2 (0.1 % in H_2O) before elution solution (80 % acetonitrile, 0.1 % TFA solution 1) was added. The assembly was centrifuged briefly to facilitate contact between peptides and elution solution and incubated for 2 min. The elution was completed by centrifugation. The eluted peptides were dried down in a SpeedVac and re-dissolved in loading solution for LC-MS/MS.

2.7.3 **LC-MS/MS**

Analysis of the peptides was carried out in a Q-Exactive hybrid quadrupole-orbitrap LC-MS/MS (Thermo Scientific Bremen, Germany) with nanoelectrospray ionization. Chromatographic separation of 1 µg peptides was conducted in a trap column (Acclaim PepMap100, C18, 5 µm, 100 Å, 300 µm i.d. ´ 5 mm) coupled to a 50 cm analytical column (Acclaim PepMap RSLC C18, 2 µm, 100 Å, 75 µm i.d. ´ 50 cm, nanoViper) with an elution gradient. The mobile phase consisted of 80 % acetonitrile and 0.1 % formic acid, and in the timespan of 120 minutes, a gradient from 4 to 40 % of this solution was used to achieve peptide separation. The flow rate was set to 300 nl/min. The LC-MS/MS was set to the Top12 method which included a full scan of 70.000 resolution (at m/z 300-1600) and 12 MS2 scans of 35000 resolution. The NCE setting used was 28 eV. Precursors with 1 charge or more than 5 were excluded for MS/MS. The dynamic exclusion of precursors was set to 20 sec.

2.7.4 **Proteomics processing**

The software platform MaxQuant (v. 1.6.3.3) was used for computational analysis of the proteomics data. The genomes used for protein identification were an inhouse sequence of *E. coli* DH5α - Rif^R and the P1 genomes MH445380.1 and MH445381.1. The former P1 genome contains transposon Tn*21*. The Perseus software (v. 1.6.5.0) was used for quality filtering and heatmap creation.

2.8 Data analysis

2.8.1 **Calculation of generation time**

Generation time (*G*) is expressed as a relation between number of generations (*n*) and the time (*t*) needed to reach this number of generations: $G = \frac{t}{n}$

Bacteria grow by binary fission, and that is explained in this equation: $b = B \times 2^n$, where *b* is the number of bacterial cells in the end of a time interval, *B* is the number of bacterial cells in the beginning of the time interval, and *n* is the number of generations in this time interval.

Solving the binary fission equation for *n*:

$$\log(b) = \log(B) + nlog(2)$$

$$n = \frac{\log(b) - \log(B)}{\log(2)}$$

The calculation of *E. coli* DH5α can be found in appendix B.

2.8.2 Absolute and relative quantification using standard curves

Copy number calculations were done using standard curves generated by qPCR measurements of DNA dilutions of each gene of interest. The number of copies was calculated using equation 1. The amount of each gene amplicon was determined by Qubit. The equation assumes one gene copy per cell, and an average base pair weight of 650 g/mole.

Equation 1

$$Number\ of\ copies = \frac{amount\ of\ amplicon\ (ng) \times 6.022 \times 10^{23} molecules/mole}{(amplicon\ length\ (bp) \times 650\ g/mole) \times 1 \times 10^{9} ng/g}$$

Standard curves showing Cq values as a function of log copy number was made for all the genes. By the use of the equation of a standard curve for a specific gene, the Cq value measured for that gene in a sample could be converted to log copy number. Equation 2 is that of the standard curve, and equation 3 is the result of a rearrangement of equation 2.

Equation 2

$$Cq = slope \times \log copy\ number + Cq\ intercept$$

Equation 3

$$\log copy\ number = \frac{Cq - Cq\ intercept}{slope}$$

The amplification efficiency of each designed primer and 16S rRNA gene primer was determined by equation 4.

Equation 4

$$Amplification\ efficiency = (10^{\frac{-1}{slope}} - 1) \times 100\ \%$$

A relative quantification of copy numbers was done using 16S rRNA gene as reference gene. Copy number relative to the 16S rRNA gene is the ratio of copy number of interest and copy number of 16S rRNA (specific gene:16S rRNA gene).

Standard curves of all the genes used in the calculations of copy numbers are given in appendix C.

2.8.3 T-tests

Paired t-test was performed to determine the significance of bacterial growth phase on bacteriophage P1 within each temperature group. The t-tests were executed in Excel using a 95 % confidence interval.

Two-sample t-tests were performed to determine statistical significance between the two temperature groups. The t-tests on the gene and genome copy number data were performed in Excel, and the proteomics data were tested in Perseus (v. 1.6.5.0). A 95 % confidence interval was used.

2.8.4 Volcano plot

Volcano plot was generated using Perseus (v. 1.6.5.0). The p-values from two-sample t-tests were used, and the fold change (FC) between the two groups was on a $\log_2$ scale. The significance level was set to $p<0.05$ and a FC=2.

2.8.5 The Basic Local Alignment Search Tool

The Basic Local Alignment Search Tool (BLAST) was utilized through the website of NCBI https://blast.ncbi.nlm.nih.gov/Blast.cgi. The tool finds regions of similarity between a query sequence (sequence of interest) and sequences in a database. The query can be a nucleotide sequence or a protein sequence. The tool calculates the significance of similarity between the query and hits in the database.

3 RESULTS

3.1 Culture and growth characteristics of bacterial strains

Light microscopy revealed that some *E. coli* DH5α - Rif^R cells have acquired a filamentous morphology. The same morphology was observed for T16 and T30, see figure 3.1. There were not any noticeable differences between the strains or between cultures grown at different temperatures. All strain cultures contained cells of many different lengths. qPCR with specific *E. coli* primers was done as a check to verify the presence of *E. coli* in the cultures used in the experiments. The qPCR gave low Cq-values. Growth in the presence of rifampicin was another approach used for verification of the strains. The strains could grow on agar infused with 320 µl/ml rifampicin.

Figure 3.1: Light microscopy of culture grown at 37 °C. The picture shows cells from a monoculture of T16. Some cells show a higher degree of filament formation compared to other cells in the culture. The arrows indicate cells of different lengths.

The progression of *E. coli* DH5α cell growth in cultures at 37 °C was investigated by cell counts. The data resulted in a mean growth curve, and this was used for generation time estimation. The generation time of *E. coli* DH5α was estimated to be 44 minutes. See appendix B for growth curve and calculations. Further, exponential and stationary growth phase of the transconjugants and *E. coli* DH5α were determined by optical density (OD_{600}) measurements of cell cultures. The observations are visualized as growth curves in figure 3.2 and reveal that the exponential growth phase was reached about OD_{600}=0.5. The bacterial cells grown at 42 °C had a longer lag phase, and reached OD_{600}=0.5 at a later point compared to the cells grown at the optimal temperature of 37 °C. Stationary phase was

reached over night. The OD_{600} at this point for T16, T30 and *E. coli* DH5α was 5.43±0.06, 5.55±0.04 and 5.54±0.11 for the cultures incubated 37 °C, respectively, and 3.56±0.23, 4.57±0.08 and 4.19±0.5 for the cultures grown at 42 °C.

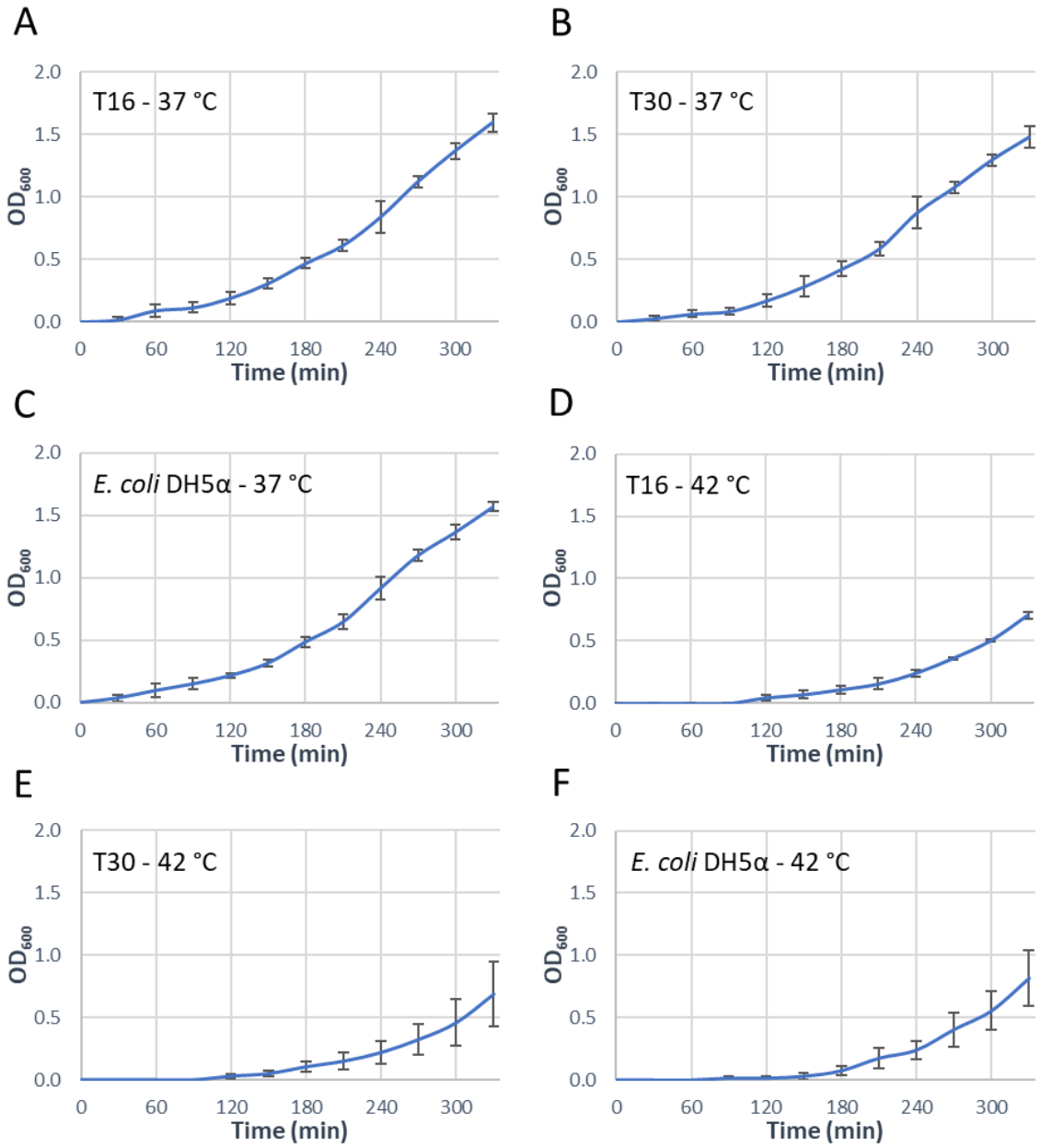

Figure 3.2: Bacterial growth curves for two incubation temperatures. Growth curve (A), (B) and (C) depict bacterial growth at 37 °C over time, using mean OD_{600} of triplicate cultures of T16, T30 and *E. coli* DH5α, respectively. Growth curve (D), (E) and (F) show bacterial growth at 42 °C over time. The mean OD_{600} is calculated from duplicate cultures of T16, T30 and *E. coli* DH5α, respectively.

The viability of the strain cultures in stationary phase at 42 °C was empirically determined using live/dead staining. About 50 % of the cells were viable. A visualization of the stained cells can be found in appendix D. Initial examination of T30 gave high Cq values when using primers for phage P1 genes. The Cq values were as high as for *E. coli* DH5α, suggesting that P1 was lost to the T30 cells. On that ground T30 was withdrawn from the experiments.

3.2 Gene expression and genome copy number

3.2.1 Primer design and optimization

Two primer pairs were designed for each of the genes *repA*, *c*1, *pcp* and *tnpA*. Optimal annealing temperature was determined by gradient PCR. Visualization of gradient PCR products on agarose gel revealed that all primers gave single bands at the expected size at all tested temperatures. See appendix E for gel results. Therefore, the same annealing temperature could be used for all primers, and this was set to 60 °C. The correlation between DNA dilutions of a specific gene and the measured Cq values was determined for all primers by qPCR. Purified PCR amplicons of the genes *repA*, *c*1, *pcp* and *tnpA* were used to make DNA dilutions. The correlation was R^2=0.99 and the amplification efficiency was close to 100 % for all the primers. The same was done for the PRK primer using dilutions of purified 16S rRNA amplicons, resulting in a standard curve with R^2=0.99 and 69 % amplification efficiency. All the standard curves are listed in appendix A. Results from HRM analysis showed that the melting point of each amplicon was the same in every qPCR run.

3.2.2 Optimizing RNA extraction protocol

Initially, most of the Cq values of the RNA eluates were below 26, suggesting DNA contamination. To optimize the DNA removal from RNA eluates, the effect of an additional DNase treatment was tested. After the treatment, the Cq values increased considerably, the lowest being 32. Cq values from the qPCR runs of RNA eluates derived from T16 are listed in appendix F.

3.2.3 Effect of growth phase and temperature on phage P1

In the stable transconjugant (T16), Cq values indicated changes in phage P1 transcription between the growth phases and cultivation temperatures. Copy numbers of the phage P1 and Tn*21* genes (*repA*, *c*1, *pcp* and *tnpA*) in each sample were calculated and made relative to 16S rRNA. Mean copy number relative to 16S rRNA of all genes were estimated. Statistical significance within temperature groups were determined in a paired t-test, and a two-sample t-test was used to calculate significance between temperature groups. The results generated with primer pair 1 are depicted in figure 3.3. As shown, the mean relative copy number of all the P1 and Tn*21* genes increased significantly in stationary phase in the cell cultures incubated at 42 °C, compared to stationary cells at 37 °C. There was also a significant increase of mean relative copy number of *repA* and *c*1 per cell in stationary phase compared to exponential phase at 42 ºC. Appendix G contain the results generated for primer pair 2.

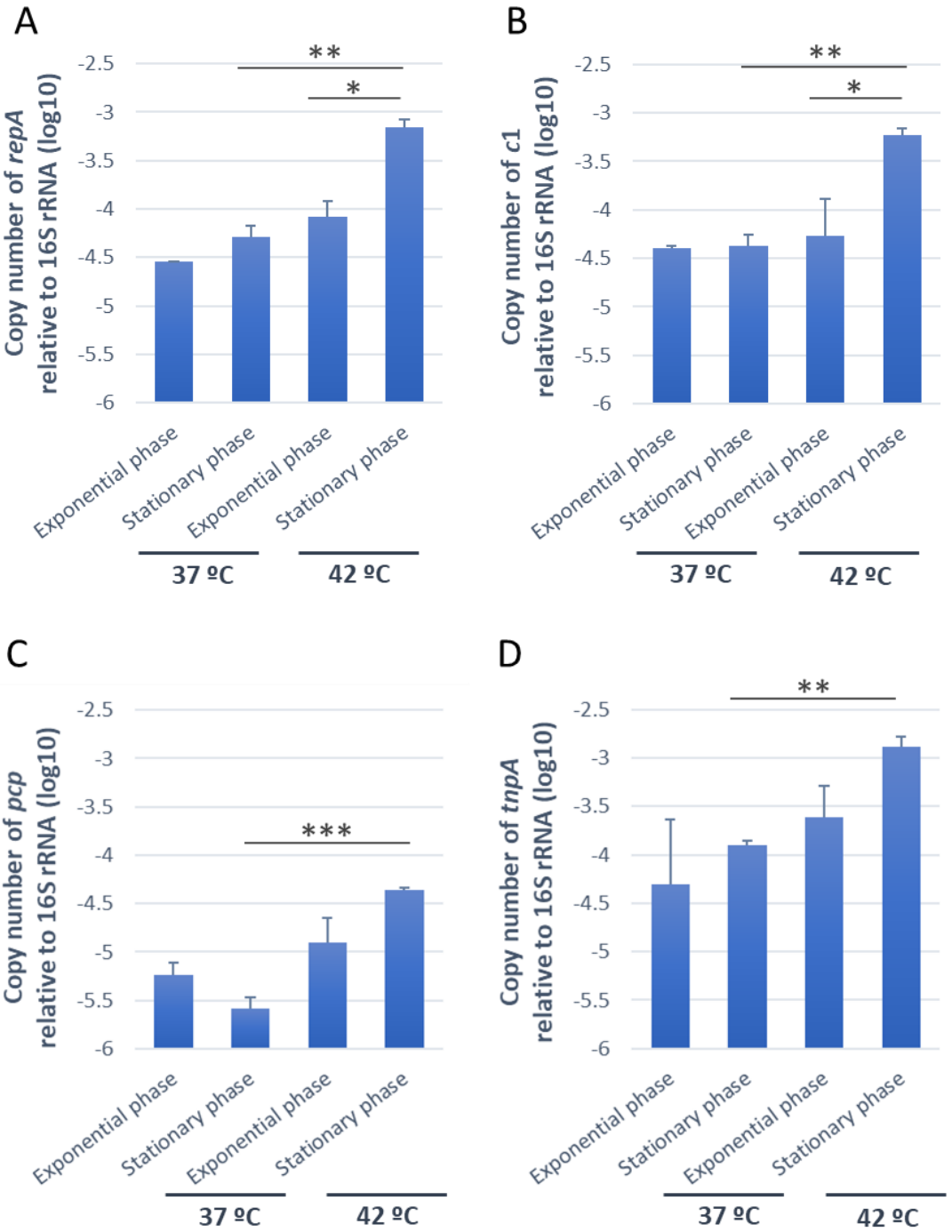

Figure 3.3: Effect of growth phase and temperature on phage P1 transcription. Schematic diagrams of phage P1 transcription of P1 and Tn*21* genes in T16 during exponential and stationary bacterial growth phase, cultivated at both 37 ºC and 42 ºC. The effect is shown as copy number relative to 16S rRNA of (A) the *repA* replication protein A gene, (B) the *c*1 repressor gene, (C) the phage capsid protein (*pcp*) gene and (D) the *tnpA* transposase gene. The values are the mean of triplicates and are log transformed. The standard deviations of the values are indicated. Primer pair 1 is used. *p<0.05, **p<0.01 and ***p<0.001.

3.2.4 Effect of temperature on phage P1 copy number

Since all of the P1 related genes in T16 were overexpressed in stationary phase at 42 ºC, it was investigated whether this could be related to the copy number of phage P1. A non-significant tendency of phage P1 genome amplification, calculated by a two-sample t-test, could be observed in stationary phase at 42 ºC. This is illustrated in figure 3.4. Primer pair 1 is used. The *repA* copy number (figure 3.4 a) show a high increase with a p-value of 0.06, which is close to the set significance level, but not significant. Calculated p-values for *c*1, *pcp* and *tnpA* copy numbers ranged from 0.1-0.3. Schematic diagrams of P1 copy numbers generated by primer pair 2 is to be found in appendix H.

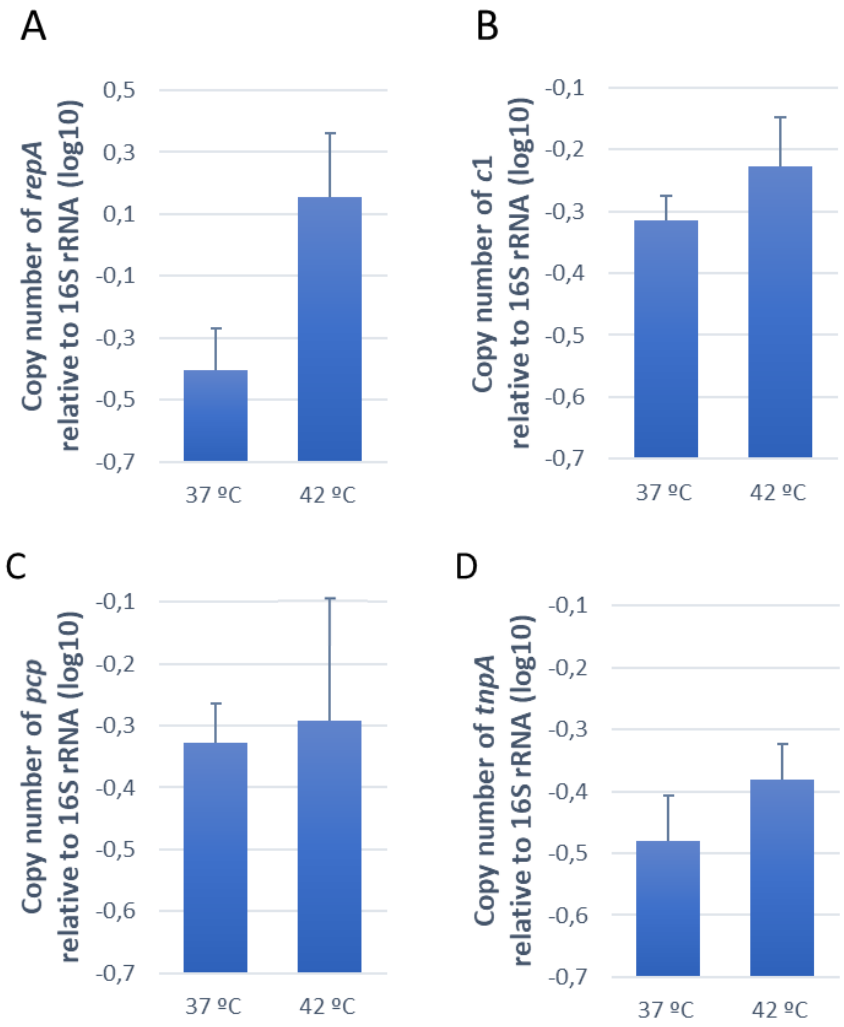

Figure 3.4: Effect of cultivation temperature on phage P1 copy number. Schematic diagrams of copy number relative to 16S rRNA of phage P1 related genes in T16 at stationary growth phase at 37 ºC and 42 ºC. The genes shown are (A) *repA* replication protein A gene, (B) *c*1 repressor gene, (C) phage capsid protein (*pcp*) gene and (D) *tnpA* transposase gene. Notise that the axis in (A) deviates from the other diagrams. The increase that can be observed in P1 copy number is not significant in any of the diagrams. The values are log transformed means of triplicates, and the standard deviations are indicated. Primer pair 1 is used.

3.3 Proteome analysis

The proteome analysis was performed on T16 grown at 37 ºC and 42 ºC. Samples were collected in stationary phase. The analysis resulted in 1346 identified proteins, and a great majority, among them the SOS response regulator LexA, originated from *E. coli* DH5α. Of all the proteins, 11 derived from phage P1. In a two-sample t-test, five of the P1 proteins showed a significant difference between the two cultivation temperatures. The 11 proteins from phage P1 are listed in table 3.1, which in addition to protein name and accession number, provides information from the protein identification process and two-sample t-test. Five of the proteins in the table have just one accession number. They were only identified by the MH445380.1 phage genome. The MH445381.1 genome did not contain the genes encoding for these proteins.

A BLAST search of all the 11 P1 related proteins was performed. The hypothetical protein resembling C1 repressor got several hits of the C1 repressor, all with E value=0.0 and 99 % identity. Streptomycin 3-O-adenylyltransferase (AXN57520.1) got a hit of the protein streptothricin acetyltransferase (E value=0.0 and 100 % identity).

Table 3.1: Proteins identified in the proteome analysis originating from phage P1. The table shows the 11 identified P1 proteins and the number of peptides that mapped to each protein in total, as well as the number of unique peptides that only mapped to these specific proteins. The sequence coverage describes how many percent of the protein that is covered by the peptides. Some proteins have two accession numbers because their respective genes occured in both P1 genomes used for identification.

Protein name	Accession	Peptides	Unique peptides	Sequence coverage
Beta-lactamase	AXN57509.1	12	12	65.0 %
Chromosome (plasmid) partitioning protein A*	AXN57571.1/ AXN57461.1	18	18	63.9 %
Chromosome (plasmid) partitioning protein B	AXN57570.1/ AXN57460.1	8	8	35.7 %
Dihydropteroate synthase	AXN57514.1	10	10	67.0 %
Hypothetical protein ASCH resembling domain[a]*	AXN57596.1/ AXN57485.1	6	6	42.7 %
Hypothetical protein resembling C1 repressor*	AXN57613.1/ AXN57502.1	23	23	72.1 %
PmgP (putative morphogenetic function)	AXN57592.1/ AXN57481.1	6	6	6.0 %
Putative outer membrane lipoprotein*	AXN57562.1/ AXN57450.1	6	6	78.3 %
Short chain dehydrogenase	AXN57513.1	12	12	69.3 %
Streptomycin 3-O-adenylyltransferase	AXN57518.1	6	6	32.8 %
Streptomycin 3-O-adenylyltransferase[b]*	AXN57520.1	24	24	71.6 %

* Significant in a two-sample t-test. $p<0.05$

[a] Significantly upregulated at 42 ºC based on volcano plot.

[b] A BLAST search gave hits of the protein streptothricin acetyltransferase, indicating an error in the protein annotation.

After statistical testing of the 1346 proteins using volcano plot, 72 proteins showed significant difference ($p<0.05$ and FC=2) in expression between the two temperature groups. 71 of these were proteins synthesized by *E. coli* DH5α. There was not detected any heat shock proteins among these, and neither was LexA.

The heatmap in figure 3.5 visualize the protein expression of the 11 P1 proteins in the two temperature groups. Only one of the P1 proteins was found to be differently regulated with statistical significance when a volcano plot of the 1346 proteins was made, and that was

the hypothetical protein containing an ASCH resembling domain. This protein is downregulated but is significantly upregulated at 42 ºC compared to 37 ºC. As shown, the C1 resembling protein is upregulated in the two groups, and there can be seen a slight increase in upregulation at 42 ºC. The increase is not significant in the volcano plot. Streptomycin 3-O-adenylyltransferase (AXN57520.1) shows high degree of upregulation at both temperatures.

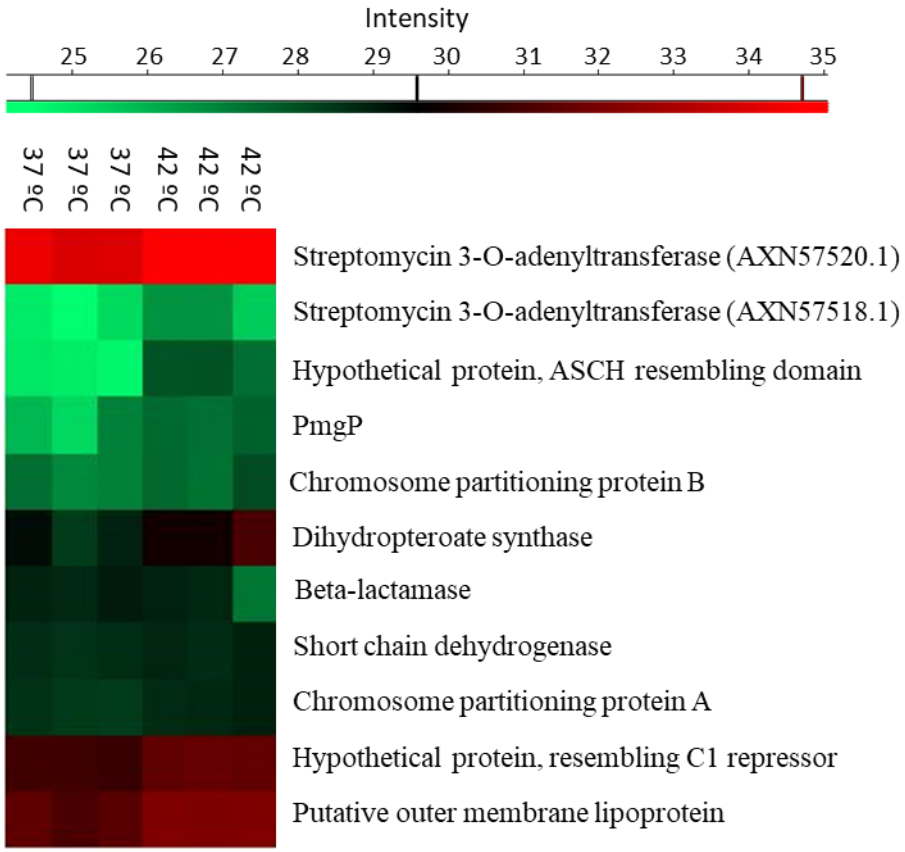

Figure 3.5: Heatmap of the P1 proteins identified by proteome analysis. The heatmap shows upregulations (red) and downregulations (green) in expression of P1 derived proteins at 37 ºC and 42 ºC. The colour intensity indicates the degree of expression. The figure shows the triplicates in each temperature group.

4 DISCUSSION

4.1 Stationary growth at 42 ºC as potential trigger of prophage induction

P1 lysogens grown at 42 ºC showed significantly increased levels of *c*1 copy number relative to 16S rRNA gene in stationary phase (figure 3.3 b), both when comparing to lysogens at 37 ºC and lysogens in the exponential phase at 42 ºC. One of the hypothetical proteins had 23 peptides, in which all of them were unique, and 71 % sequence coverage in the proteome analysis, supporting the identification. This protein got hits of the C1 repressor in a BLAST search, and it is therefore likely to assume that the identified hypothetical protein is the C1 repressor of bacteriophage P1. Further, the proteome analysis revealed that expression of this C1 resembling protein was upregulated at 37 ºC (figure 3.5), which is in consistency with lysogenic growth of the bacteriophage. A non-significant trend of C1 upregulation was detected in stationary phase lysogens at 42 ºC compared to 37 ºC. In a study performed by Heinzel *et al.* (1990), a raise in *c*1 expression was observed as a response to *coi* expression. The Coi inactivation of C1 lead to immediate increased C1 synthesis as the C1 autorepression was abolished (Heinzel *et al.*, 1990). Based on this, the increased *c*1 expression observed in this thesis might be due to derepression of the *c*1 gene operator, which can be a consequence of Coi synthesis. Heinzel *et al.* (1990) further suggested that prophage induction could be caused by Coi synthesis because of Coi's ability to derepress lytic functions. Transcription of *coi* has been proposed to be regulated by the transcriptional repressor LexA (Lobocka *et al.*, 2004). LexA is a repressor of the bacterial SOS response and gets inactivated by cleavage, leading to expression of SOS responses (Little *et al.*, 1980). A LexA binding site has been found to overlap the predicted promoter region upstream of the *coi* gene in the P1 genome, indicating induction of *coi* transcription upon LexA inactivation (Lewis *et al.*, 1994; Lobocka *et al.*, 2004). Despite findings that might imply *coi* synthesis, the Coi protein was not identified in this work. This result might be due to expression below detection level of the proteome analysis. The LexA protein, however, was identified, but there was no detectable difference in expression. The analysis may not be able to distinguish between active LexA, and LexA that has been inactivated by cleavage. Taking previous research into consideration, together with the current finding of increased *c*1 expression, elevated cultivation temperature and stationary growth phase

may induce the lytic state of wild-type bacteriophage P1. A potential model for the early phase of P1 prophage induction is depicted in figure 4.1.

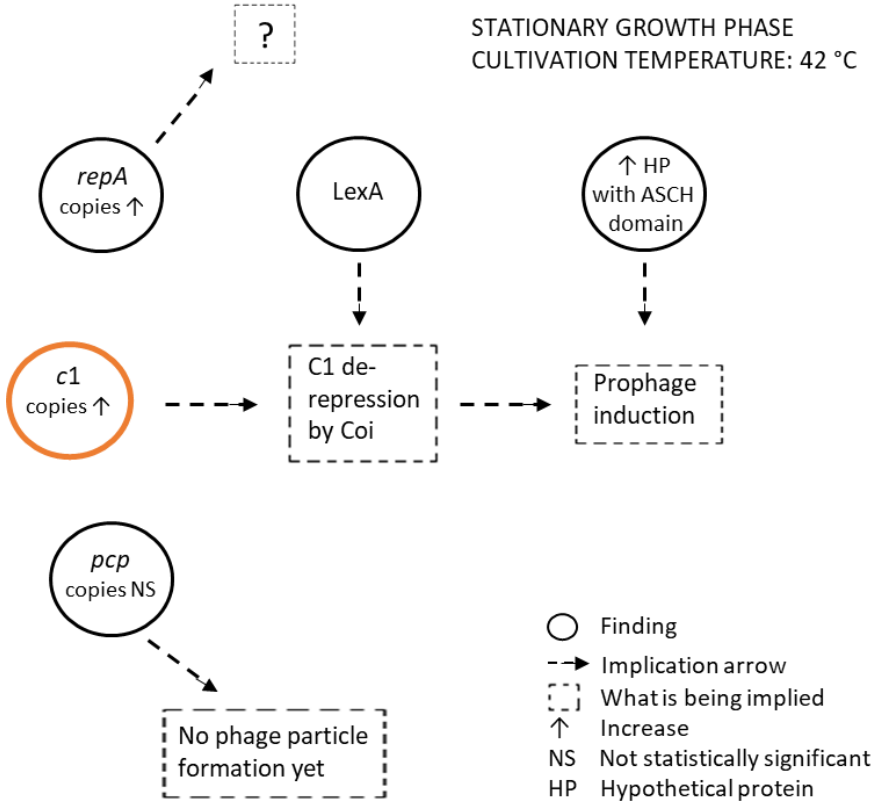

Figure 4.1: Model of an early stage of P1 prophage induction. Based on findings in this thesis, a model of the early stage of P1 prophage induction is proposed. The model is centralized around the increase of *c*1 repressor gene expression at 42 ºC. It illustrates possible implications of this observation, with support from expression of *pcp* phage capsid protein gene, *repA* replication protein A gene, LexA repressor protein and hypothetical protein with an ASCH resembling domain. The model depicts a state in which the prophage changes the expression of lysogenic genes (*c*1 and *repA*) and the hypothetical protein, while expression of late genes of lytic replication (*pcp*) remains unchanged. It is proposed that the increase in *c*1 copy number is a response to C1 derepression of the Coi antirepressor protein. LexA may be involved in Coi synthesis. As Coi is a driver of lytic gene expression that further implies that the prophage is induced.

A significant increase in *repA* copy number relative to 16S rRNA was observed in stationary phase lysogens at 42 ºC (figure 3.3 a), compared to lysogens at 37 ºC and lysogens in exponential phase at 42 ºC. It is anticipated that the degree of transcription of an autoregulated gene varies as the cell grow, to keep up the concentration of the protein (Norris, 1995). In order to accomplish initiation of replication, the RepA concentration needs to reach a threshold. Consequently, the rate of transcription is at its highest when the

cell has grown and is on the verge of cell division. However, it seems unlikely that this transcription hypothesis can explain the differences observed in *repA* copy number level. Replication needs to be performed either the cell is in exponential or stationary phase, and the event happens at equal rates. A potential interpretation of the significant elevated number of *repA* transcripts may be that the genome replication in stationary phase lysogens at 42 ºC is upregulated. However, the finding of non-significant difference in P1 genome copy number in stationary phase when comparing the two temperatures (figure 3.4) suggests that this is not the case. The difference in genome copy numbers generated by the *repA*_1_F/R primers (figure 3.4 a) was found to be close to the set significance level. A potential explanation for the increase might be that a portion of the cells in the cell cultures was executing genome replication. *oriR* is situated close to the *repA* gene. As the two genomes get synthesized during replication, the *repA* gene is represented on each genome from the beginning of replication, while other genes further away from *oriR* exist twice for a shorter period. This might explain why the *repA* copy number is higher than for the other genes. Interestingly, RepA was not found in the proteome analysis, but the plasmid partitioning proteins ParA and ParB were identified. All these proteins are involved to ensure preservation of the phage in the bacterial cell line, and therefore the absence of RepA in the proteomics results was unexpected. A possible explanation for this might be that the RepA concentration was too low to be detected in the analysis. Considering the strict regulation of *repA* transcription, the increase in *repA* copy number is quite striking. It is difficult to give an explanation for the increase based on the *repA* regulation model. Too little information about P1 prophage induction is known to comprehend the observed raise in *repA* copy number, but it is plausible that this result is a response to a) the elevated temperature the lysogens are exposed to and b) the physiological conditions in the lysogens caused by stationary growth. The possibility of this result to be a sign of lytic state activation should not be ruled out, considering the previously discussed aspects of *c*1 copy number and their implications for lytic functions.

pcp copy number relative to 16S rRNA was significantly higher in P1 lysogens at 42 ºC compared to 37 ºC in stationary phase (figure 3.3 c). There was a non-significant difference of the matter regarding lysogens in exponential and stationary phase. These findings indicate that *pcp* transcription remains repressed in stationary phase of the lysogens, which is consistent with the proteome analysis results. No *pcp* encoded proteins were discovered in the proteome analysis. That further implies that no occurrence of phage particle

formation has taken place, since the *pcp* encoded protein is a constituent of the phage capsid. The significant increase in copy number in stationary phase between the two temperatures may be due to a lapse in regulation of the gene. The results for *pcp* in this work are compatible with the previous debated suggestions of a prophage induction supported by the observed *c*1 expression. As previously elaborated, the increase in *c*1 copy number may suggest that the phage is observed in a stage of prophage induction. *pcp* and other structural genes belong to the late genes of bacteriophages, meaning that they are expressed after lytic replication. With that in mind, the absence of *pcp* expression does not necessarily exclude the possibility of achieved activation of lytic functions in the lysogens. It might imply that P1 is in an early phase of prophage induction.

The hypothetical protein with an ASCH resembling domain was significantly upregulated at 42 ºC compared to 37 ºC (figure 3.5). ASCH domains have been proposed to be involved in transcriptional coactivation and regulation of translation (Iyer *et al.*, 2006), and an ASCH containing protein has been found to degrade ssRNA (Kim *et al.*, 2017). Little information exists on the identified hypothetical protein, but the presence of the ASCH resembling domain may suggest that it is involved in one of the mentioned processes. Possibly as a driver of prophage induction.

The current findings indicate that the P1 prophage is affected by temperature and physiological state of its bacterial host. Even though the results might imply prophage induction, there were not detected any signs of lytic activity in form of increased transcription of capsid proteins or identified proteins involved in lytic functions. A possible explanation might be that the P1 phage is induced by the unfavourable conditions of the host but is unable to carry out lytic growth at the current physiological state of its host. Lytic growth has been found to be dependent on bacterial growth rate and the availability of the bacterial machinery used for phage particle formation, favouring lytic growth (Golec *et al.*, 2014; Hadas *et al.*, 1997). A previous study showed that few phage particles were released from cells in stationary phase, but when the conditions improved by addition of nutrients, the phage production exploded (Middelboe, 2000). In the light of this research, the observation of increased *c*1 copy number in the P1 lysogens might be compatible with the absence of phage particles in stationary phase. Another possible function of the hypothetical protein containing an ASCH resembling domain may be regulation of the prophage induction state, not allowing the phage to enter lytic growth until the physiology

of the host changes. It is plausible that the P1 prophage is induced, possibly preparing for environmental changes that favours bacterial growth.

4.2 Stationary growth at 42 ºC as potential trigger of Tn*21* translocation

In this study, *tnpA* copy number relative to 16S rRNA was found to be significantly higher in stationary phase lysogens at 42 ºC compared to the lysogens at 37 ºC (figure 3.3 d). This result is consistent with previous studies that have found transposases to be temperature sensitive and that translocation happens more frequently at 42 ºC (Haren *et al.*, 1997; Ohtsubo *et al.*, 2005). When comparing the two growth phases at 42 ºC, the difference in *tnpA* copy number is not significant, implying that growth phase does not have the same inducing effect as temperature on the matter. Haren *et al.* (1997) found that regulation of transposase decreased gradually with an increase in temperature from 30 ºC to 42 ºC. An implication of this is that the human gut, holding 37 ºC, or a human gut holding temperatures above 37 ºC due to fever, is an inducer of transposition of transposons and other transposase-containing genetic elements. This can contribute to the dissemination of AR genes if these are accessory genes of the MGEs. Even though a raise in *tnpA* copy number was detected, no TnpA proteins were identified. The P1 phage in this thesis was found to synthesise proteins that only the transposon containing P1 genome encoded for. This suggests that these proteins derive from transposon Tn*21*. One of the streptomycin 3-O-adenylyltransferase proteins identified did significantly resemble the AR protein streptothricin acetyltransferase, indicating an error in the annotation of this protein in the MH445380.1 genome. In addition to these proteins, a third AR protein, beta-lactamase, was detected. It is worth noticing that the streptomycin 3-O-adenylyltransferase protein that resembled streptothricin acetyltransferase showed high degree of upregulation (figure 3.5) at both temperatures. Taking into account that the lysogens not were put under antibiotic pressure, this finding is quite striking. The Tn*21* transposon in this work derives from the gut of a preterm infant. Considering the observed level of *tnpA* transcription, it is plausible that Tn*21* can translocate between MGEs in the infant gut microbiota and disseminate AR genes through horizontal gene transfer. It is alarming that AR genes that are highly expressed in bacteria grown at 37 ºC without the presence of antibiotics may spread among bacteria in the infant gut.

4.3 The relation between bacteriophage P1 and transposon Tn*21*

Translocation of Tn*21* to bacteriophage P1 has been seen i*n vitro* (Hagbø, 2017), and the current findings imply that its transposase can be active in conditions like the human gut. Although this work was unable to detect P1 transmission, the possibility of transmission in the gut microbiota should not be excluded. P1 transmission has occurred before *in vitro* (Hagbø, 2017), and the current work has shown that stationary growth at temperatures above optimum of the lysogens may cause prophage induction. Regardless of this, P1-like phages carrying AR genes have been characterized from clinical isolates (Billard-Pomares *et al.*, 2014) and domestic animal isolates (Yang *et al.*, 2017), and as part of the floating genome, bacteriophage P1 may contribute to dissemination of AR genes. Tn*21* may be involved in this process.

4.4 Methodological considerations

Studying the P1 phage in the laboratory strain *E. coli* DH5α - Rif^R may be a limitation of the study as the strain might have mutations that could affect the bacteriophage. The cells are developed to become resistant to rifampicin and have probably acquired a filamentous morphology because of that, and the physiology of these cells might have impacted the results (Fux *et al.*, 2005). However, the extensive knowledge that exists on laboratory strains has made them suitable for laboratory experiments, and they are therefore widely used (Blount, 2015).

The standard curves used in quantification was based on purified DNA amplicons while the actual samples investigated were more complex. They consisted of cDNA derived from all RNA extracted from the cells. Efficiency and accuracy of qPCR depend on DNA quality, and in quantification the amplification efficiencies of sample and standard should be the same (Brankatschk *et al.*, 2012). The quantification performed in this thesis might have been compromised since the amplification efficiency of cDNA samples not has been determined.

Regarding the relative quantification of copy numbers using a reference gene, the amplification efficiencies of target gene and reference gene should be approximately equal (Livak & Schmittgen, 2001). The amplification efficiency of the reference gene was below that of the target genes, due to the large amplicon size (Debode *et al.*, 2017). Nonetheless, the 16S rRNA gene was chosen because it is a well-studied housekeeping gene and widely used as a reference gene (Sun *et al.*, 2017; Takle *et al.*, 2007; Wang, S. *et al.*, 2009).

The results generated by primer pair 2 (appendix G, figure G.1, and appendix H, figure H.1) show a bigger variance between replicates than the results generated by primer pair 1 (figure 3.3 and 3.4). Therefore, the results from primer pair 1 was chosen. Some of the same trends can be seen in the results from both primer pairs, yet, the differences that these pairs create should be investigated further in future studies.

5 CONCLUSION AND FURTHER RESEARCH

A significant increase in *c*1 copy number at the elevated temperature in stationary phase lysogens was found, suggesting that prophage induction has occurred. A protein resembling the C1 repressor was identified. The C1 antirepressor Coi was not identified. Significant increase in *repA* copy number was detected under the same conditions as for *c*1, but unfortunately, we cannot provide a reasonable explanation for this. There was a non-significant raise in *pcp* copy number between exponential and stationary phase at the elevated temperature and no phage particle proteins were identified, indicating that phage particle production not had taken place. A hypothetical protein with an ASCH resembling domain, possibly involved in transcription and translation, was significantly upregulated at the elevated temperature compared to the optimal temperature.

When comparing optimal and elevated growth temperature, the *tnpA* copy number was higher at the latter one, suggesting that *tnpA* expression in Tn*21* is temperature sensitive. Several antibiotic resistance proteins were found expressed from the Tn*21* transposon, and one of them were upregulated at both temperatures.

The infant gut microbiota is suggested to be a reservoir for MGEs and AR genes, and its relevance in the multidrug resistance development needs to be established. The current work has provided new insight regarding circumstances that induce the wild-type P1 prophage and its involvement in dissemination of AR genes. To bridge the gaps between P1 immunity, prophage induction and lytic growth, future studies should investigate the roles of antirepressor Coi and its putative repressor LexA during prophage inducing conditions. The function of the hypothetical protein containing the ASCH resembling domain should also be established. In addition, the impact accelerated bacterial growth might have on the P1 prophage after a period of stationary growth may contribute to a better understanding of the activation of lytic functions.

References

Ackermann, H. W. & Prangishvili, D. (2012). Prokaryote viruses studied by electron microscopy. *Archives of Virology*, 157 (10): 1843-1849. doi: 10.1007/s00705-012-1383-y.

Austin, S., Ziese, M. & Sternberg, N. (1981). A novel role for site-specific recombination in maintenance of bacterial replicons. *Cell*, 25 (3): 729-36.

Backhed, F., Roswall, J., Peng, Y., Feng, Q., Jia, H., Kovatcheva-Datchary, P., Li, Y., Xia, Y., Xie, H., Zhong, H., et al. (2015). Dynamics and Stabilization of the Human Gut Microbiome during the First Year of Life. *Cell Host Microbe*, 17 (5): 690-703. doi: 10.1016/j.chom.2015.04.004.

Bertani, G. (1951). Studies on lysogenesis. I. The mode of phage liberation by lysogenic Escherichia coli. *J Bacteriol*, 62 (3): 293-300.

Billard-Pomares, T., Fouteau, S., Jacquet, M. E., Roche, D., Barbe, V., Castellanos, M., Bouet, J. Y., Cruveiller, S., Médigue, C., Blanco, J., et al. (2014). Characterization of a P1-Like Bacteriophage Carrying an SHV-2 Extended-Spectrum β-Lactamase from an Escherichia coli Strain. *Antimicrobial Agents and Chemotherapy*, 58 (11): 6550-6557. doi: 10.1128/AAC.03183-14.

Blount, Z. D. (2015). The unexhausted potential of E. coli. *Elife*, 4. doi: 10.7554/eLife.05826.

Bondy-Denomy, J., Qian, J., Westra, E. R., Buckling, A., Guttman, D. S., Davidson, A. R. & Maxwell, K. L. (2016). Prophages mediate defense against phage infection through diverse mechanisms. *ISME J*, 10 (12): 2854-2866. doi: 10.1038/ismej.2016.79.

Brankatschk, R., Bodenhausen, N., Zeyer, J. & Burgmann, H. (2012). Simple absolute quantification method correcting for quantitative PCR efficiency variations for microbial community samples. *Appl Environ Microbiol*, 78 (12): 4481-9. doi: 10.1128/AEM.07878-11.

Breitbart, M., Hewson, I., Felts, B., Mahaffy, J. M., Nulton, J., Salamon, P. & Rohwer, F. (2003). Metagenomic analyses of an uncultured viral community from human feces. *J Bacteriol*, 185 (20): 6220-3.

Breitbart, M., Haynes, M., Kelley, S., Angly, F., Edwards, R. A., Felts, B., Mahaffy, J. M., Mueller, J., Nulton, J., Rayhawk, S., et al. (2008). Viral diversity and dynamics in an infant gut. *Res Microbiol*, 159 (5): 367-73. doi: 10.1016/j.resmic.2008.04.006.

Broaders, E., Gahan, C. G. & Marchesi, J. R. (2013). Mobile genetic elements of the human gastrointestinal tract: potential for spread of antibiotic resistance genes. *Gut Microbes*, 4 (4): 271-80. doi: 10.4161/gmic.24627.

Brolund, A., Franzen, O., Melefors, O., Tegmark-Wisell, K. & Sandegren, L. (2013). Plasmidome-analysis of ESBL-producing escherichia coli using conventional typing and high-throughput sequencing. *PLoS One*, 8 (6): e65793. doi: 10.1371/journal.pone.0065793.

Brown, H. J., Stokes, H. W. & Hall, R. M. (1996). The integrons In0, In2, and In5 are defective transposon derivatives. *J Bacteriol*, 178 (15): 4429-37.

Burmeister, A. R. (2015). Horizontal Gene Transfer. *Evol Med Public Health*, 2015 (1): 193-4. doi: 10.1093/emph/eov018.

Bustin, S. A., Benes, V., Nolan, T. & Pfaffl, M. W. (2005). Quantitative real-time RT-PCR--a perspective. *J Mol Endocrinol*, 34 (3): 597-601. doi: 10.1677/jme.1.01755.

Candela, M., Perna, F., Carnevali, P., Vitali, B., Ciati, R., Gionchetti, P., Rizzello, F., Campieri, M. & Brigidi, P. (2008). Interaction of probiotic Lactobacillus and Bifidobacterium strains with human intestinal epithelial cells: adhesion properties, competition against enteropathogens and modulation of IL-8 production. *Int J Food Microbiol*, 125 (3): 286-92. doi: 10.1016/j.ijfoodmicro.2008.04.012.

Carattoli, A. (2013). Plasmids and the spread of resistance. *Int J Med Microbiol*, 303 (6-7): 298-304. doi: 10.1016/j.ijmm.2013.02.001.

Casjens, S. R. & Thuman-Commike, P. A. (2011). Evolution of mosaically related tailed bacteriophage genomes seen through the lens of phage P22 virion assembly. *Virology*, 411 (2): 393-415. doi: 10.1016/j.virol.2010.12.046.
Cenens, W., Makumi, A., Mebrhatu, M. T., Lavigne, R. & Aertsen, A. (2013). Phage-host interactions during pseudolysogeny: Lessons from the Pid/dgo interaction. *Bacteriophage*, 3 (1): e25029. doi: 10.4161/bact.25029.
Chan, B. K., Abedon, S. T. & Loc-Carrillo, C. (2013). Phage cocktails and the future of phage therapy. *Future Microbiol*, 8 (6): 769-83. doi: 10.2217/fmb.13.47.
Chattoraj, D. K., Mason, R. J. & Wickner, S. H. (1988). Mini-P1 plasmid replication: the autoregulation-sequestration paradox. *Cell*, 52 (4): 551-7.
Chattoraj, D. K. (2000). Control of plasmid DNA replication by iterons: no longer paradoxical. *Mol Microbiol*, 37 (3): 467-76.
Chern, E. C., Siefring, S., Paar, J., Doolittle, M. & Haugland, R. A. (2011). Comparison of quantitative PCR assays for Escherichia coli targeting ribosomal RNA and single copy genes. *Lett Appl Microbiol*, 52 (3): 298-306. doi: 10.1111/j.1472-765X.2010.03001.x.
Choi, J. D., Kotay, S. M. & Goel, R. (2010). Various physico-chemical stress factors cause prophage induction in Nitrosospira multiformis 25196-an ammonia oxidizing bacteria. *Water Research*, 44 (15): 4550-4558. doi: 10.1016/j.watres.2010.04.040.
Choi, K. H. (2012). Viral Polymerases. *Viral Molecular Machines*, 726: 267-304. doi: 10.1007/978-1-4614-0980-9_12.
Citron, M. & Schuster, H. (1990). The c4 repressors of bacteriophages P1 and P7 are antisense RNAs. *Cell*, 62 (3): 591-8.
Cohen, G. (1983). Electron microscopy study of early lytic replication forms of bacteriophage P1 DNA. *Virology*, 131 (1): 159-70.
Comeau, A. M., Hatfull, G. F., Krisch, H. M., Lindell, D., Mann, N. H. & Prangishvili, D. (2008). Exploring the prokaryotic virosphere. *Research in Microbiology*, 159 (5): 306-313. doi: https://doi.org/10.1016/j.resmic.2008.05.001.
Coren, J. S., Pierce, J. C. & Sternberg, N. (1995). Headful packaging revisited: the packaging of more than one DNA molecule into a bacteriophage P1 head. *J Mol Biol*, 249 (1): 176-84. doi: 10.1006/jmbi.1995.0287.
Couturier, M. R., Lee, B., Zelyas, N. & Chui, L. (2011). Shiga-toxigenic Escherichia coli detection in stool samples screened for viral gastroenteritis in Alberta, Canada. *J Clin Microbiol*, 49 (2): 574-8. doi: 10.1128/JCM.01693-10.
Cuskin, F., Lowe, E. C., Temple, M. J., Zhu, Y., Cameron, E., Pudlo, N. A., Porter, N. T., Urs, K., Thompson, A. J., Cartmell, A., et al. (2015). Human gut Bacteroidetes can utilize yeast mannan through a selfish mechanism. *Nature*, 517 (7533): 165-169. doi: 10.1038/nature13995.
Debode, F., Marien, A., Janssen, E., Bragard, C. & Berben, G. (2017). The influence of amplicon length on real-time PCR results. *Biotechnologie Agronomie Societe Et Environnement*, 21 (1): 3-11.
Domingues, S., da Silva, G. J. & Nielsen, K. M. (2012). Integrons: Vehicles and pathways for horizontal dissemination in bacteria. *Mob Genet Elements*, 2 (5): 211-223. doi: 10.4161/mge.22967.
Dong, F., Zhang, Y., Yao, K., Lu, J., Guo, L., Lyu, S., Yang, Y., Wang, Y., Zheng, H., Song, W., et al. (2018). Epidemiology of Carbapenem-Resistant Klebsiella pneumoniae Bloodstream Infections in a Chinese Children's Hospital: Predominance of New Delhi Metallo-beta-Lactamase-1. *Microb Drug Resist*, 24 (2): 154-160. doi: 10.1089/mdr.2017.0031.
Doss, J., Culbertson, K., Hahn, D., Camacho, J. & Barekzi, N. (2017). A Review of Phage Therapy against Bacterial Pathogens of Aquatic and Terrestrial Organisms. *Viruses*, 9 (3). doi: 10.3390/v9030050.
Eckburg, P. B., Bik, E. M., Bernstein, C. N., Purdom, E., Dethlefsen, L., Sargent, M., Gill, S. R., Nelson, K. E. & Relman, D. A. (2005). Diversity of the human intestinal microbial flora. *Science*, 308 (5728): 1635-8. doi: 10.1126/science.1110591.

Edwards, K. J. & Saunders, N. A. (2001). Real-time PCR used to measure stress-induced changes in the expression of the genes of the alginate pathway of Pseudomonas aeruginosa. *J Appl Microbiol*, 91 (1): 29-37.
Encarnacion-Guevara, S. (2017). The dawn and the first twenty-five years of proteomics in Mexico: a personal chronicle. *Bol Med Hosp Infant Mex*, 74 (3): 208-211. doi: 10.1016/j.bmhimx.2017.03.006.
Forsberg, K. J., Reyes, A., Wang, B., Selleck, E. M., Sommer, M. O. & Dantas, G. (2012). The shared antibiotic resistome of soil bacteria and human pathogens. *Science*, 337 (6098): 1107-11. doi: 10.1126/science.1220761.
Fukuda, S., Toh, H., Hase, K., Oshima, K., Nakanishi, Y., Yoshimura, K., Tobe, T., Clarke, J. M., Topping, D. L., Suzuki, T., et al. (2011). Bifidobacteria can protect from enteropathogenic infection through production of acetate. *Nature*, 469 (7331): 543-7. doi: 10.1038/nature09646.
Fux, C. A., Shirtliff, M., Stoodley, P. & Costerton, J. W. (2005). Can laboratory reference strains mirror 'real-world' pathogenesis? *Trends in Microbiology*, 13 (2): 58-63. doi: 10.1016/j.tim.2004.11.001.
Ghafourian, S., Sadeghifard, N., Soheili, S. & Sekawi, Z. (2015). Extended Spectrum Beta-lactamases: Definition, Classification and Epidemiology. *Curr Issues Mol Biol*, 17: 11-21.
Golec, P., Karczewska-Golec, J., Los, M. & Wegrzyn, G. (2014). Bacteriophage T4 can produce progeny virions in extremely slowly growing Escherichia coli host: comparison of a mathematical model with the experimental data. *FEMS Microbiol Lett*, 351 (2): 156-61. doi: 10.1111/1574-6968.12372.
Govindarajan, R., Duraiyan, J., Kaliyappan, K. & Palanisamy, M. (2012). Microarray and its applications. *J Pharm Bioallied Sci*, 4 (Suppl 2): S310-2. doi: 10.4103/0975-7406.100283.
Guo, J. (2014). Transcription: the epicenter of gene expression. *J Zhejiang Univ Sci B*, 15 (5): 409-11. doi: 10.1631/jzus.B1400113.
Hadas, H., Einav, M., Fishov, I. & Zaritsky, A. (1997). Bacteriophage T4 development depends on the physiology of its host Escherichia coli. *Microbiology*, 143 (Pt 1): 179-85. doi: 10.1099/00221287-143-1-179.
Hagbø, M. E. S. (2017). *Characterization of conjugative plasmids in the gut microbiota from a preterm twin pair*: Norwegian University of Life Sciences.
Hall, R. M. & Collis, C. M. (1995). Mobile gene cassettes and integrons: capture and spread of genes by site-specific recombination. *Mol Microbiol*, 15 (4): 593-600.
Hamady, M. & Knight, R. (2009). Microbial community profiling for human microbiome projects: Tools, techniques, and challenges. *Genome Res*, 19 (7): 1141-52. doi: 10.1101/gr.085464.108.
Haren, L., Betermier, M., Polard, P. & Chandler, M. (1997). IS911-mediated intramolecular transposition is naturally temperature sensitive. *Mol Microbiol*, 25 (3): 531-40.
Hatfull, G. F. & Hendrix, R. W. (2011). Bacteriophages and their genomes. *Curr Opin Virol*, 1 (4): 298-303. doi: 10.1016/j.coviro.2011.06.009.
Heinrich, J., Citron, M., Gunther, A. & Schuster, H. (1994). Second-site suppressors of the bacteriophage P1 virs mutant reveal the interdependence of the c4, icd, and ant genes in the P1 immI operon. *J Bacteriol*, 176 (16): 4931-6.
Heinrich, J., Velleman, M. & Schuster, H. (1995). The tripartite immunity system of phages P1 and P7. *FEMS Microbiol Rev*, 17 (1-2): 121-6. doi: 10.1111/j.1574-6976.1995.tb00193.x.
Heinzel, T., Velleman, M. & Schuster, H. (1990). The c1 repressor inactivator protein coi of bacteriophage P1. Cloning and expression of coi and its interference with c1 repressor function. *J Biol Chem*, 265 (29): 17928-34.
Heinzel, T., Velleman, M. & Schuster, H. (1992). C1 repressor of phage P1 is inactivated by noncovalent binding of P1 Coi protein. *J Biol Chem*, 267 (6): 4183-8.
Horcajadas, J. A., Monsalve, M., Rojo, F. & Salas, M. (1999). The switch from early to late transcription in phage GA-1: characterization of the regulatory protein p4G. *J Mol Biol*, 290 (5): 917-28. doi: 10.1006/jmbi.1999.2932.

Howard-Varona, C., Hargreaves, K. R., Abedon, S. T. & Sullivan, M. B. (2017). Lysogeny in nature: mechanisms, impact and ecology of temperate phages. *Isme Journal*, 11 (7): 1511-1520. doi: 10.1038/ismej.2017.16.

Huddleston, J. R. (2014). Horizontal gene transfer in the human gastrointestinal tract: potential spread of antibiotic resistance genes. *Infect Drug Resist*, 7: 167-76. doi: 10.2147/IDR.S48820.

Ioannou, P. A., Amemiya, C. T., Garnes, J., Kroisel, P. M., Shizuya, H., Chen, C., Batzer, M. A. & de Jong, P. J. (1994). A new bacteriophage P1-derived vector for the propagation of large human DNA fragments. *Nat Genet*, 6 (1): 84-9. doi: 10.1038/ng0194-84.

Iyer, L. M., Burroughs, A. M. & Aravind, L. (2006). The ASCH superfamily: novel domains with a fold related to the PUA domain and a potential role in RNA metabolism. *Bioinformatics*, 22 (3): 257-63. doi: 10.1093/bioinformatics/bti767.

Johnston, C., Martin, B., Fichant, G., Polard, P. & Claverys, J. P. (2014). Bacterial transformation: distribution, shared mechanisms and divergent control. *Nat Rev Microbiol*, 12 (3): 181-96. doi: 10.1038/nrmicro3199.

Kapitan, M., Niemiec, M. J., Steimle, A., Frick, J. S. & Jacobsen, I. D. (2018). Fungi as Part of the Microbiota and Interactions with Intestinal Bacteria. *Curr Top Microbiol Immunol*. doi: 10.1007/82_2018_117.

Karam, M. R. A., Habibi, M. & Bouzari, S. (2019). Urinary tract infection: Pathogenicity, antibiotic resistance and development of effective vaccines against Uropathogenic Escherichia coli. *Molecular Immunology*, 108: 56-67. doi: 10.1016/j.molimm.2019.02.007.

Karpievitch, Y. V., Polpitiya, A. D., Anderson, G. A., Smith, R. D. & Dabney, A. R. (2010). Liquid Chromatography Mass Spectrometry-Based Proteomics: Biological and Technological Aspects. *Ann Appl Stat*, 4 (4): 1797-1823. doi: 10.1214/10-AOAS341.

Kim, B. N., Shin, M., Ha, S. C., Park, S. Y., Seo, P. W., Hofmann, A. & Kim, J. S. (2017). Crystal structure of an ASCH protein from Zymomonas mobilis and its ribonuclease activity specific for single-stranded RNA. *Sci Rep*, 7 (1): 12303. doi: 10.1038/s41598-017-12186-w.

Lavysh, D., Sokolova, M., Slashcheva, M., Forstner, K. U. & Severinov, K. (2017). Transcription Profiling of Bacillus subtilis Cells Infected with AR9, a Giant Phage Encoding Two Multisubunit RNA Polymerases. *MBio*, 8 (1). doi: 10.1128/mBio.02041-16.

Leiman, P. G. & Shneider, M. M. (2012). Contractile Tail Machines of Bacteriophages. *Viral Molecular Machines*, 726: 93-114. doi: 10.1007/978-1-4614-0980-9_5.

Lennox, E. S. (1955). Transduction of linked genetic characters of the host by bacteriophage P1. *Virology*, 1 (2): 190-206.

Levin, H. L. & Moran, J. V. (2011). Dynamic interactions between transposable elements and their hosts. *Nat Rev Genet*, 12 (9): 615-27. doi: 10.1038/nrg3030.

Lewis, L. K., Harlow, G. R., Gregg-Jolly, L. A. & Mount, D. W. (1994). Identification of high affinity binding sites for LexA which define new DNA damage-inducible genes in Escherichia coli. *J Mol Biol*, 241 (4): 507-23. doi: 10.1006/jmbi.1994.1528.

Ley, R. E., Lozupone, C. A., Hamady, M., Knight, R. & Gordon, J. I. (2008). Worlds within worlds: evolution of the vertebrate gut microbiota. *Nat Rev Microbiol*, 6 (10): 776-88. doi: 10.1038/nrmicro1978.

Li, B. & Webster, T. J. (2018). Bacteria antibiotic resistance: New challenges and opportunities for implant-associated orthopedic infections. *J Orthop Res*, 36 (1): 22-32. doi: 10.1002/jor.23656.

Liebert, C. A., Hall, R. M. & Summers, A. O. (1999). Transposon Tn21, flagship of the floating genome. *Microbiol Mol Biol Rev*, 63 (3): 507-22.

Lim, E. S., Zhou, Y., Zhao, G., Bauer, I. K., Droit, L., Ndao, I. M., Warner, B. B., Tarr, P. I., Wang, D. & Holtz, L. R. (2015). Early life dynamics of the human gut virome and bacterial microbiome in infants. *Nat Med*, 21 (10): 1228-34. doi: 10.1038/nm.3950.

Little, J. W., Edmiston, S. H., Pacelli, L. Z. & Mount, D. W. (1980). Cleavage of the Escherichia coli lexA protein by the recA protease. *Proc Natl Acad Sci U S A*, 77 (6): 3225-9. doi: 10.1073/pnas.77.6.3225.

Livak, K. J. & Schmittgen, T. D. (2001). Analysis of relative gene expression data using real-time quantitative PCR and the 2(-Delta Delta C(T)) Method. *Methods*, 25 (4): 402-8. doi: 10.1006/meth.2001.1262.

Lobocka, M. B., Rose, D. J., Plunkett, G., 3rd, Rusin, M., Samojedny, A., Lehnherr, H., Yarmolinsky, M. B. & Blattner, F. R. (2004). Genome of bacteriophage P1. *J Bacteriol*, 186 (21): 7032-68. doi: 10.1128/JB.186.21.7032-7068.2004.

Lozupone, C. A., Stombaugh, J. I., Gordon, J. I., Jansson, J. K. & Knight, R. (2012). Diversity, stability and resilience of the human gut microbiota. *Nature*, 489 (7415): 220-30. doi: 10.1038/nature11550.

McFall-Ngai, M., Hadfield, M. G., Bosch, T. C., Carey, H. V., Domazet-Loso, T., Douglas, A. E., Dubilier, N., Eberl, G., Fukami, T., Gilbert, S. F., et al. (2013). Animals in a bacterial world, a new imperative for the life sciences. *Proc Natl Acad Sci U S A*, 110 (9): 3229-36. doi: 10.1073/pnas.1218525110.

Middelboe, M. (2000). Bacterial Growth Rate and Marine Virus-Host Dynamics. *Microb Ecol*, 40 (2): 114-124.

Milani, C., Duranti, S., Bottacini, F., Casey, E., Turroni, F., Mahony, J., Belzer, C., Delgado Palacio, S., Arboleya Montes, S., Mancabelli, L., et al. (2017). The First Microbial Colonizers of the Human Gut: Composition, Activities, and Health Implications of the Infant Gut Microbiota. *Microbiol Mol Biol Rev*, 81 (4). doi: 10.1128/MMBR.00036-17.

Morin, R. D., Bainbridge, M., Fejes, A., Hirst, M., Krzywinski, M., Pugh, T. J., McDonald, H., Varhol, R., Jones, S. J. M. & Marra, M. A. (2008). Profiling the HeLa S3 transcriptome using randomly primed cDNA and massively parallel short-read sequencing. *Biotechniques*, 45 (1): 81-+. doi: 10.2144/000112900.

Morton, E. R., Lynch, J., Froment, A., Lafosse, S., Heyer, E., Przeworski, M., Blekhman, R. & Segurel, L. (2015). Variation in Rural African Gut Microbiota Is Strongly Correlated with Colonization by Entamoeba and Subsistence. *PLoS Genet*, 11 (11): e1005658. doi: 10.1371/journal.pgen.1005658.

Munita, J. M. & Arias, C. A. (2016). Mechanisms of Antibiotic Resistance. *Microbiology spectrum*, 4 (2): 10.1128/microbiolspec.VMBF-0016-2015. doi: 10.1128/microbiolspec.VMBF-0016-2015.

Nadkarni, M. A., Martin, F. E., Jacques, N. A. & Hunter, N. (2002). Determination of bacterial load by real-time PCR using a broad-range (universal) probe and primers set. *Microbiology*, 148 (Pt 1): 257-66. doi: 10.1099/00221287-148-1-257.

Naito, M. & Pawlowska, T. E. (2016). The role of mobile genetic elements in evolutionary longevity of heritable endobacteria. *Mob Genet Elements*, 6 (1): e1136375. doi: 10.1080/2159256X.2015.1136375.

Nanda, A. M., Heyer, A., Kramer, C., Grunberger, A., Kohlheyer, D. & Frunzke, J. (2014). Analysis of SOS-induced spontaneous prophage induction in Corynebacterium glutamicum at the single-cell level. *J Bacteriol*, 196 (1): 180-8. doi: 10.1128/JB.01018-13.

Normanno, D., Dahan, M. & Darzacq, X. (2012). Intra-nuclear mobility and target search mechanisms of transcription factors: a single-molecule perspective on gene expression. *Biochim Biophys Acta*, 1819 (6): 482-93. doi: 10.1016/j.bbagrm.2012.02.001.

Norris, V. (1995). Hypothesis: transcriptional sensing and membrane-domain formation initiate chromosome replication in Escherichia coli. *Mol Microbiol*, 15 (5): 985-7.

O'Connor, C., Philip, R. K., Kelleher, J., Powell, J., O'Gorman, A., Slevin, B., Woodford, N., Turton, J. F., McGrath, E., Finnegan, C., et al. (2017). The first occurrence of a CTX-M ESBL-producing Escherichia coli outbreak mediated by mother to neonate transmission in an Irish neonatal intensive care unit. *BMC Infect Dis*, 17 (1): 16. doi: 10.1186/s12879-016-2142-6.

OECD. (2018). *Stemming the Superbug Tide: Just A Few Dollars More*. OECD Health Policy Studies: OECD Publishing, Paris.

Ohtsubo, Y., Genka, H., Komatsu, H., Nagata, Y. & Tsuda, M. (2005). High-temperature-induced transposition of insertion elements in burkholderia multivorans ATCC 17616. *Appl Environ Microbiol*, 71 (4): 1822-8. doi: 10.1128/AEM.71.4.1822-1828.2005.

Oli, A. N., Eze, D. E., Gugu, T. H., Ezeobi, I., Maduagwu, U. N. & Ihekwereme, C. P. (2017). Multi-antibiotic resistant extended-spectrum beta-lactamase producing bacteria pose a challenge to the effective treatment of wound and skin infections. *Pan Afr Med J*, 27: 66. doi: 10.11604/pamj.2017.27.66.10226.

Olson, M. E. (2016). Bacteriophage Transduction in Staphylococcus aureus. *Methods Mol Biol*, 1373: 69-74. doi: 10.1007/7651_2014_186.

Olszak, T., An, D., Zeissig, S., Vera, M. P., Richter, J., Franke, A., Glickman, J. N., Siebert, R., Baron, R. M., Kasper, D. L., et al. (2012). Microbial exposure during early life has persistent effects on natural killer T cell function. *Science*, 336 (6080): 489-93. doi: 10.1126/science.1219328.

Osborne, F. A., Stovall, S. R. & Baumstark, B. R. (1989). The c1 genes of P1 and P7. *Nucleic Acids Res*, 17 (19): 7671-80. doi: 10.1093/nar/17.19.7671.

Osbourn, A. E. & Field, B. (2009). Operons. *Cell Mol Life Sci*, 66 (23): 3755-75. doi: 10.1007/s00018-009-0114-3.

Oveland, E., Muth, T., Rapp, E., Martens, L., Berven, F. S. & Barsnes, H. (2015). Viewing the proteome: how to visualize proteomics data? *Proteomics*, 15 (8): 1341-55. doi: 10.1002/pmic.201400412.

Pal, S. K., Mason, R. J. & Chattoraj, D. K. (1986). P1 plasmid replication. Role of initiator titration in copy number control. *J Mol Biol*, 192 (2): 275-85.

Papp-Wallace, K. M., Endimiani, A., Taracila, M. A. & Bonomo, R. A. (2011). Carbapenems: past, present, and future. *Antimicrob Agents Chemother*, 55 (11): 4943-60. doi: 10.1128/AAC.00296-11.

Park, J. J., Seo, Y. B. & Lee, J. (2017). Antimicrobial Susceptibilities of Enterobacteriaceae in Community-Acquired Urinary Tract Infections during a 5-year Period: A Single Hospital Study in Korea. *Infect Chemother*, 49 (3): 184-193. doi: 10.3947/ic.2017.49.3.184.

Partridge, S. R., Kwong, S. M., Firth, N. & Jensen, S. O. (2018). Mobile Genetic Elements Associated with Antimicrobial Resistance. *Clin Microbiol Rev*, 31 (4). doi: 10.1128/CMR.00088-17.

Penders, J., Stobberingh, E. E., Savelkoul, P. H. & Wolffs, P. F. (2013). The human microbiome as a reservoir of antimicrobial resistance. *Front Microbiol*, 4: 87. doi: 10.3389/fmicb.2013.00087.

Pierce, J. C. & Sternberg, N. L. (1992). Using bacteriophage P1 system to clone high molecular weight genomic DNA. *Methods Enzymol*, 216: 549-74.

Pitout, J. D., Nordmann, P., Laupland, K. B. & Poirel, L. (2005). Emergence of Enterobacteriaceae producing extended-spectrum beta-lactamases (ESBLs) in the community. *J Antimicrob Chemother*, 56 (1): 52-9. doi: 10.1093/jac/dki166.

Rao, R., Bing Zhu, Y., Alinejad, T., Tiruvayipati, S., Lin Thong, K., Wang, J. & Bhassu, S. (2015). RNA-seq analysis of Macrobrachium rosenbergii hepatopancreas in response to Vibrio parahaemolyticus infection. *Gut Pathog*, 7: 6. doi: 10.1186/s13099-015-0052-6.

Ravi, A., Avershina, E., Foley, S. L., Ludvigsen, J., Storrø, O., Øien, T., Johnsen, R., McCartney, A. L., L'Abée-Lund, T. M. & Rudi, K. (2015). The commensal infant gut meta-mobilome as a potential reservoir for persistent multidrug resistance integrons. *Scientific Reports*, 5: 15317. doi: 10.1038/srep15317.

Ravi, A., Estensmo, E. L. F., Abée-Lund, T. M. L., Foley, S. L., Allgaier, B., Martin, C. R., Claud, E. C. & Rudi, K. (2017). Association of the gut microbiota mobilome with hospital location and birth weight in preterm infants. *Pediatric Research*, 82: 829. doi: 10.1038/pr.2017.146.

Rizzo, L., Manaia, C., Merlin, C., Schwartz, T., Dagot, C., Ploy, M. C., Michael, I. & Fatta-Kassinos, D. (2013). Urban wastewater treatment plants as hotspots for antibiotic resistant bacteria and genes spread into the environment: a review. *Sci Total Environ*, 447: 345-60. doi: 10.1016/j.scitotenv.2013.01.032.

Ruiz, L., Moles, L., Gueimonde, M. & Rodriguez, J. M. (2016). Perinatal Microbiomes' Influence on Preterm Birth and Preterms' Health: Influencing Factors and Modulation Strategies. *J Pediatr Gastroenterol Nutr*, 63 (6): e193-e203. doi: 10.1097/MPG.0000000000001196.

Schaefer, T. S. & Hays, J. B. (1990). The bof gene of bacteriophage P1: DNA sequence and evidence for roles in regulation of phage c1 and ref genes. *J Bacteriol*, 172 (6): 3269-77.
Segundo-Val, I. S. & Sanz-Lozano, C. S. (2016). Introduction to the Gene Expression Analysis. *Methods Mol Biol*, 1434: 29-43. doi: 10.1007/978-1-4939-3652-6_3.
Shah, J., Jefferies, A. L., Yoon, E. W., Lee, S. K., Shah, P. S. & Canadian Neonatal, N. (2015). Risk Factors and Outcomes of Late-Onset Bacterial Sepsis in Preterm Neonates Born at < 32 Weeks' Gestation. *Am J Perinatol*, 32 (7): 675-82. doi: 10.1055/s-0034-1393936.
Sharma, S., Chatterjee, S., Datta, S., Prasad, R., Dubey, D., Prasad, R. K. & Vairale, M. G. (2017). Bacteriophages and its applications: an overview. *Folia Microbiologica*, 62 (1): 17-55. doi: 10.1007/s12223-016-0471-x.
Shintani, M., Sanchez, Z. K. & Kimbara, K. (2015). Genomics of microbial plasmids: classification and identification based on replication and transfer systems and host taxonomy. *Front Microbiol*, 6: 242. doi: 10.3389/fmicb.2015.00242.
Smeal, S. W., Schmitt, M. A., Pereira, R. R., Prasad, A. & Fisk, J. D. (2017). Simulation of the M13 life cycle I: Assembly of a genetically-structured deterministic chemical kinetic simulation. *Virology*, 500: 259-274. doi: 10.1016/j.virol.2016.08.017.
Smillie, C., Garcillán-Barcia, M. P., Francia, M. V., Rocha, E. P. C. & de la Cruz, F. (2010). Mobility of Plasmids. *Microbiology and Molecular Biology Reviews : MMBR*, 74 (3): 434-452. doi: 10.1128/MMBR.00020-10.
Sonnenburg, J. L., Xu, J., Leip, D. D., Chen, C.-H., Westover, B. P., Weatherford, J., Buhler, J. D. & Gordon, J. I. (2005). Glycan Foraging in Vivo by an Intestine-Adapted Bacterial Symbiont. *Science*, 307 (5717): 1955-1959. doi: 10.1126/science.1109051.
Sternberg, N. (1990). Bacteriophage P1 cloning system for the isolation, amplification, and recovery of DNA fragments as large as 100 kilobase pairs. *Proc Natl Acad Sci U S A*, 87 (1): 103-7. doi: 10.1073/pnas.87.1.103.
Sternberg, N., Ruether, J. & deRiel, K. (1990). Generation of a 50,000-member human DNA library with an average DNA insert size of 75-100 kbp in a bacteriophage P1 cloning vector. *New Biol*, 2 (2): 151-62.
Sun, Z., Deng, J., Wu, H., Wang, Q. & Zhang, Y. (2017). Selection of Stable Reference Genes for Real-Time Quantitative PCR Analysis in Edwardsiella tarda. *J Microbiol Biotechnol*, 27 (1): 112-121. doi: 10.4014/jmb.1605.05023.
Tacconelli, E., Carrara, E., Savoldi, A., Harbarth, S., Mendelson, M., Monnet, D. L., Pulcini, C., Kahlmeter, G., Kluytmans, J., Carmeli, Y., et al. (2018). Discovery, research, and development of new antibiotics: the WHO priority list of antibiotic-resistant bacteria and tuberculosis. *Lancet Infect Dis*, 18 (3): 318-327. doi: 10.1016/S1473-3099(17)30753-3.
Takeuchi, O. & Akira, S. (2009). Innate immunity to virus infection. *Immunol Rev*, 227 (1): 75-86. doi: 10.1111/j.1600-065X.2008.00737.x.
Takle, G. W., Toth, I. K. & Brurberg, M. B. (2007). Evaluation of reference genes for real-time RT-PCR expression studies in the plant pathogen Pectobacterium atrosepticum. *BMC Plant Biol*, 7: 50. doi: 10.1186/1471-2229-7-50.
Tschudin-Sutter, S., Frei, R., Battegay, M., Hoesli, I. & Widmer, A. F. (2010). Extended spectrum ss-lactamase-producing Escherichia coli in neonatal care unit. *Emerg Infect Dis*, 16 (11): 1758-60. doi: 10.3201/eid1611.100366.
Turnbaugh, P. J., Ley, R. E., Hamady, M., Fraser-Liggett, C. M., Knight, R. & Gordon, J. I. (2007). The human microbiome project. *Nature*, 449 (7164): 804-10. doi: 10.1038/nature06244.
Vandecasteele, S. J., Peetermans, W. E., Merckx, R. & Van Eldere, J. (2001). Quantification of expression of Staphylococcus epidermidis housekeeping genes with Taqman quantitative PCR during in vitro growth and under different conditions. *J Bacteriol*, 183 (24): 7094-101. doi: 10.1128/JB.183.24.7094-7101.2001.
Vihta, K. D., Stoesser, N., Llewelyn, M. J., Quan, T. P., Davies, T., Fawcett, N. J., Dunn, L., Jeffery, K., Butler, C. C., Hayward, G., et al. (2018). Trends over time in Escherichia coli bloodstream infections, urinary tract infections, and antibiotic susceptibilities in Oxfordshire, UK, 1998-2016: a study of electronic health records. *Lancet Infect Dis*, 18 (10): 1138-1149. doi: 10.1016/S1473-3099(18)30353-0.

von Wintersdorff, C. J., Penders, J., Stobberingh, E. E., Oude Lashof, A. M., Hoebe, C. J., Savelkoul, P. H. & Wolffs, P. F. (2014). High rates of antimicrobial drug resistance gene acquisition after international travel, The Netherlands. *Emerg Infect Dis*, 20 (4): 649-57. doi: 10.3201/eid.2004.131718.

Wang, S., Deng, K., Zaremba, S., Deng, X., Lin, C., Wang, Q., Tortorello, M. L. & Zhang, W. (2009). Transcriptomic response of Escherichia coli O157:H7 to oxidative stress. *Appl Environ Microbiol*, 75 (19): 6110-23. doi: 10.1128/AEM.00914-09.

Wang, Z., Gerstein, M. & Snyder, M. (2009). RNA-Seq: a revolutionary tool for transcriptomics. *Nat Rev Genet*, 10 (1): 57-63. doi: 10.1038/nrg2484.

Weinbauer, M. G. (2004). Ecology of prokaryotic viruses. *FEMS Microbiol Rev*, 28 (2): 127-81. doi: 10.1016/j.femsre.2003.08.001.

Wittebole, X., De Roock, S. & Opal, S. M. (2014). A historical overview of bacteriophage therapy as an alternative to antibiotics for the treatment of bacterial pathogens. *Virulence*, 5 (1): 226-35. doi: 10.4161/viru.25991.

Xu, M., Hu, L., Huang, H., Wang, L., Tan, J., Zhang, Y., Chen, C., Zhang, X. & Huang, L. (2019). Etiology and Clinical Features of Full-Term Neonatal Bacterial Meningitis: A Multicenter Retrospective Cohort Study. *Front Pediatr*, 7: 31. doi: 10.3389/fped.2019.00031.

Yang, L., Li, W., Jiang, G. Z., Zhang, W. H., Ding, H. Z., Liu, Y. H., Zeng, Z. L. & Jiang, H. X. (2017). Characterization of a P1-like bacteriophage carrying CTXM-27 in Salmonella spp. resistant to third generation cephalosporins isolated from pork in China (vol 7, 40710, 2017). *Scientific Reports*, 7. doi: ARTN 4672810.1038/srep46728.

Zhang, Z., Li, J., Zheng, W., Zhao, G., Zhang, H., Wang, X., Guo, Y., Qin, C. & Shi, Y. (2016). Peripheral Lymphoid Volume Expansion and Maintenance Are Controlled by Gut Microbiota via RALDH+ Dendritic Cells. *Immunity*, 44 (2): 330-42. doi: 10.1016/j.immuni.2016.01.004.

Zhao, Y., Su, J. Q., Ye, J., Rensing, C., Tardif, S., Zhu, Y. G. & Brandt, K. K. (2019). AsChip: A High-Throughput qPCR Chip for Comprehensive Profiling of Genes Linked to Microbial Cycling of Arsenic. *Environ Sci Technol*, 53 (2): 798-807. doi: 10.1021/acs.est.8b03798.

Zilberberg, M. D., Nathanson, B. H., Sulham, K., Fan, W. & Shorr, A. F. (2017). Carbapenem resistance, inappropriate empiric treatment and outcomes among patients hospitalized with Enterobacteriaceae urinary tract infection, pneumonia and sepsis. *BMC Infect Dis*, 17 (1): 279. doi: 10.1186/s12879-017-2383-z.

Zougman, A., Selby, P. J. & Banks, R. E. (2014). Suspension trapping (STrap) sample preparation method for bottom-up proteomics analysis. *Proteomics*, 14 (9): 1006-0. doi: 10.1002/pmic.201300553.

Appendix

Appendix A: Growth medium and solutions

LB agar/broth (400 ml)

4 g Tryptose (Merck)

4 g NaCl (VWR)

2 g yeast extract (Merck)

6 g agar* (VWR)

400 ml H_2O

*For LB broth, leave out the agar

PBS (1x, 1 L, pH 7.4)

8 g NaCl

200 mg KCl

1.44 g Na2HPO4

240 mg KH2PO4

1 L H_2O

Appendix B: Calculation of *E. coli* DH5α generation time

Values used in the *E. coli* DH5α growth curve is given in table B.1. The growth curve is depicted in figure B.1. The calculation of *E. coli* DH5α is shown.

Table B.1: Number of colony forming units (CFU) per ml per hour during growth of E. coli DH5α in LB broth at 37 ºC.

Hours	Mean CFU/ml	Mean log CFU/ml
1	30.6×10^6	7.4
2	86.3×10^6	7.9
3	15.3×10^7	8.2
4	53.6×10^7	8.7
5	72.3×10^7	8.8
6	10.8×10^8	9.0
7	13.0×10^8	9.1
8	16.0×10^8	9.2
24	89.6×10^8	10.0

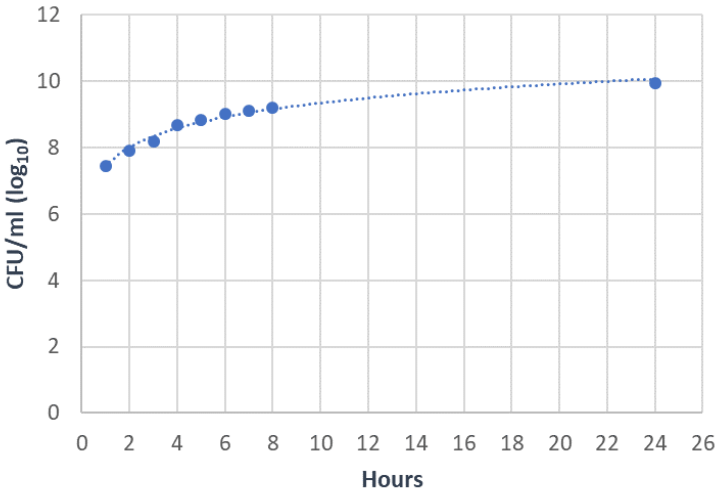

Figure B.1: Growth curve of *E. coli* DH5α. Graphic visualization of bacterial growth expressed as CFU/ml per hour. The first hour the bacterial cells are in the exponential growth phase. After 24 hour the stationary phase is reached. The values are the mean of triplicates and are log transformed.

Calculating generation time of *E. coli* DH5α:

Time interval: 1 to 4 hours
t = 180 min
B = 30.6 x 10^6 CFU/ml

b = 53.6 x 10^7 CFU/ml

$$n = \frac{\log(b) - \log(B)}{\log(2)} = \frac{\log(53.6 \text{ x } 10^7) - \log(30.6 \text{ x } 10^6)}{\log(2)} = 4.1$$

$$G = \frac{t}{n} = \frac{180\ min}{4.1} = 43.9\ min \approx 44\ min$$

Appendix C: Standard curves

Each gene has been amplified using two different sets of primers (primer pair 1 and 2). Therefore, standard curves using each of the primer pairs have been made, and these are listed in table C.1. They are all used for copy number calculations of each specific gene.

Table C1: Standard curves. Values for the standard curve equation, correlation, amplification efficiency and copy numbers are given.

Target gene	**Primer**	**Slope**	**Cq intercept**	**R^2**	**Amplification efficiency**	**Linear range (gene copies per 2 µl DNA)**
repA	repA_1_F/R	-2.93	36.2	0.99	119 %	$40.8 \times 10^2 – 40.8 \times 10^7$
	repA_2_F/R	-3.03	35.7	0.99	114 %	$10.7 \times 10^3 – 10.7 \times 10^8$
c1	c1_1_F/R	-3.10	35.8	0.99	110 %	$15.3 \times 10^3 – 15.3 \times 10^8$
	c1_2_F/R	-3.12	36.7	0.99	109 %	$82.5 \times 10^3 – 82.5 \times 10^7$
pcp	pcp_1_F/R	-3.14	36.7	0.99	108 %	$11.5 \times 10^3 – 11.5 \times 10^8$
	pcp_2_F/R	-3.37	38.9	0.99	98 %	$80.9 \times 10^2 – 80.9 \times 10^7$
tnpA	tnpA_1_F/R	-3.32	37.8	0.99	100 %	$90.2 \times 10^2 – 90.2 \times 10^7$
	tnpA_2_F/R	-3.16	36.9	0.99	107 %	$84.6 \times 10^2 – 84.6 \times 10^7$
16S rRNA	PRK341 F PRK806 R	-4.39	47.7	0.99	69 %	$92.4 \times 10^1 – 92.4 \times 10^6$

Appendix D: Visualization of cells cultivated at 42 °C

The viability of T16 cells grown at 42 °C was determined using live/dead staining. The cells are shown in figure D.1.

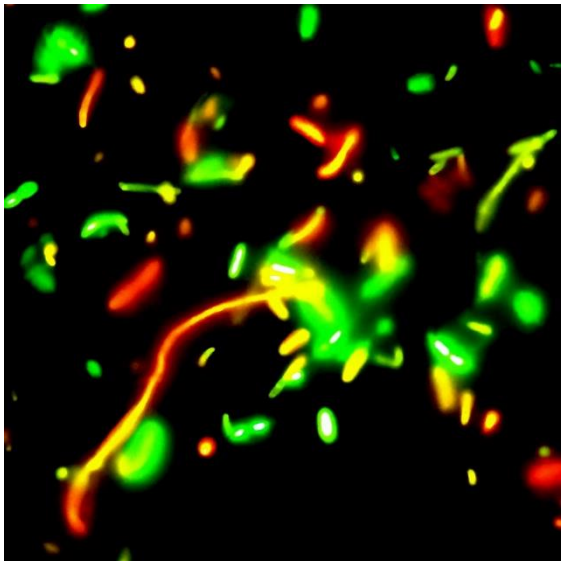

Figure D.1: Microscopy of culture grown at 42 °C using live/dead staining. The figure shows cells that are viable (green colour), dying (yellow colour) and dead (red/orange colour). The culture is a monoculture of T16, and different morphologies of the cells are represented.

Appendix E: Gel electrophoresis of gradient PCR products

Gel electrophoreses of gene fragments amplified with designed primers at different annealing temperatures are shown in figure E.1-E.4. In each well on the gel, amplicons produced with a specific annealing temperature is loaded. An overview of the annealing temperatures is given in table E.1.

Table E.1: Overview of annealing temperatures in gradient PCR. The wells in this table correspond to the wells on the gels.

Well	1	2	3	4	5	6	7	8	9	10	11	12
Degrees (ºC)	52.9	53.2	54.0	55.2	56.8	58.7	60.6	62.5	64.3	65.8	66.9	67.5

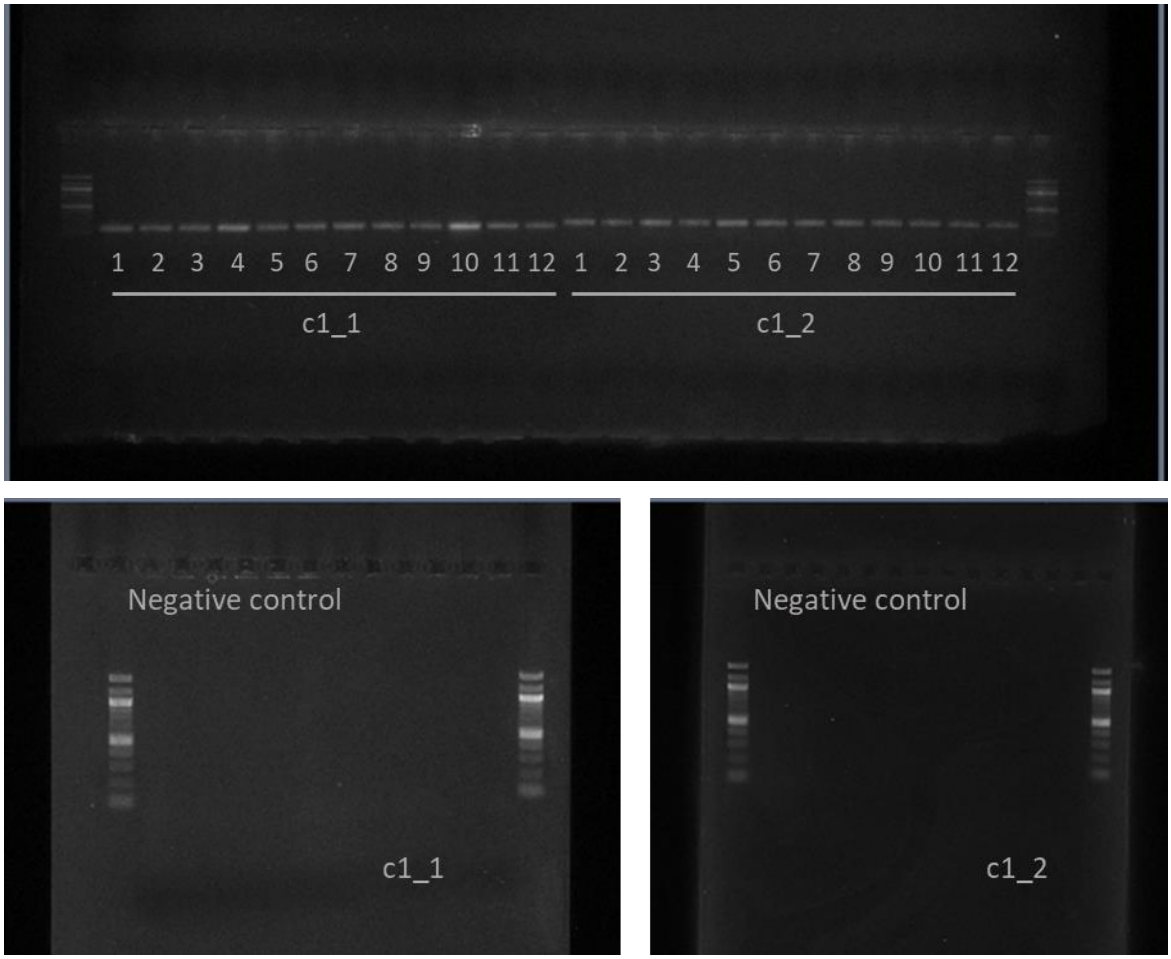

Figure E.1: Gradient PCR products and negative controls generated by c1_1_F/R and c1_2_F/R primers.

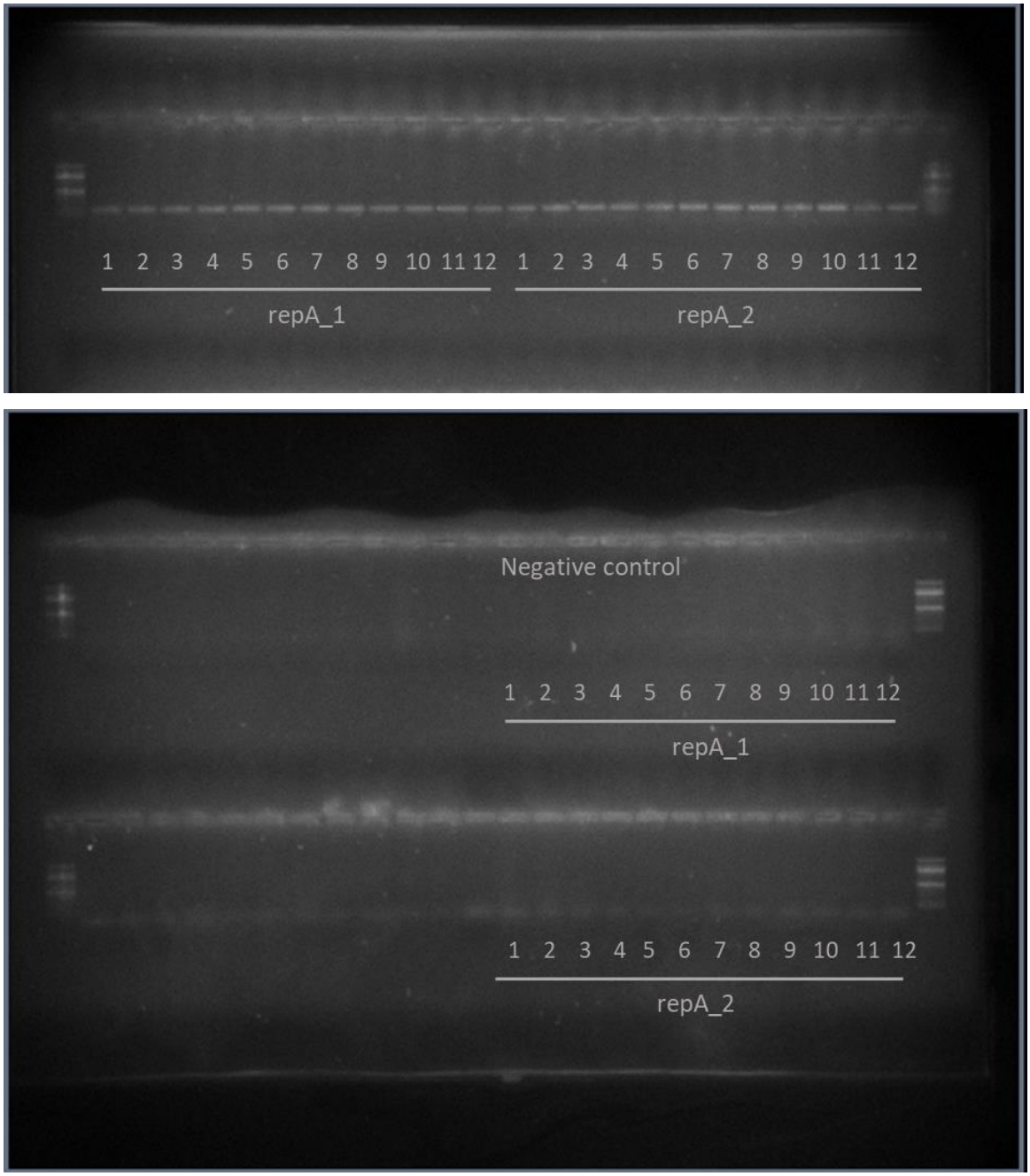

Figure E.2: Gradient PCR products and negative controls generated by repA_1_F/R and repA_2_F/R primers.

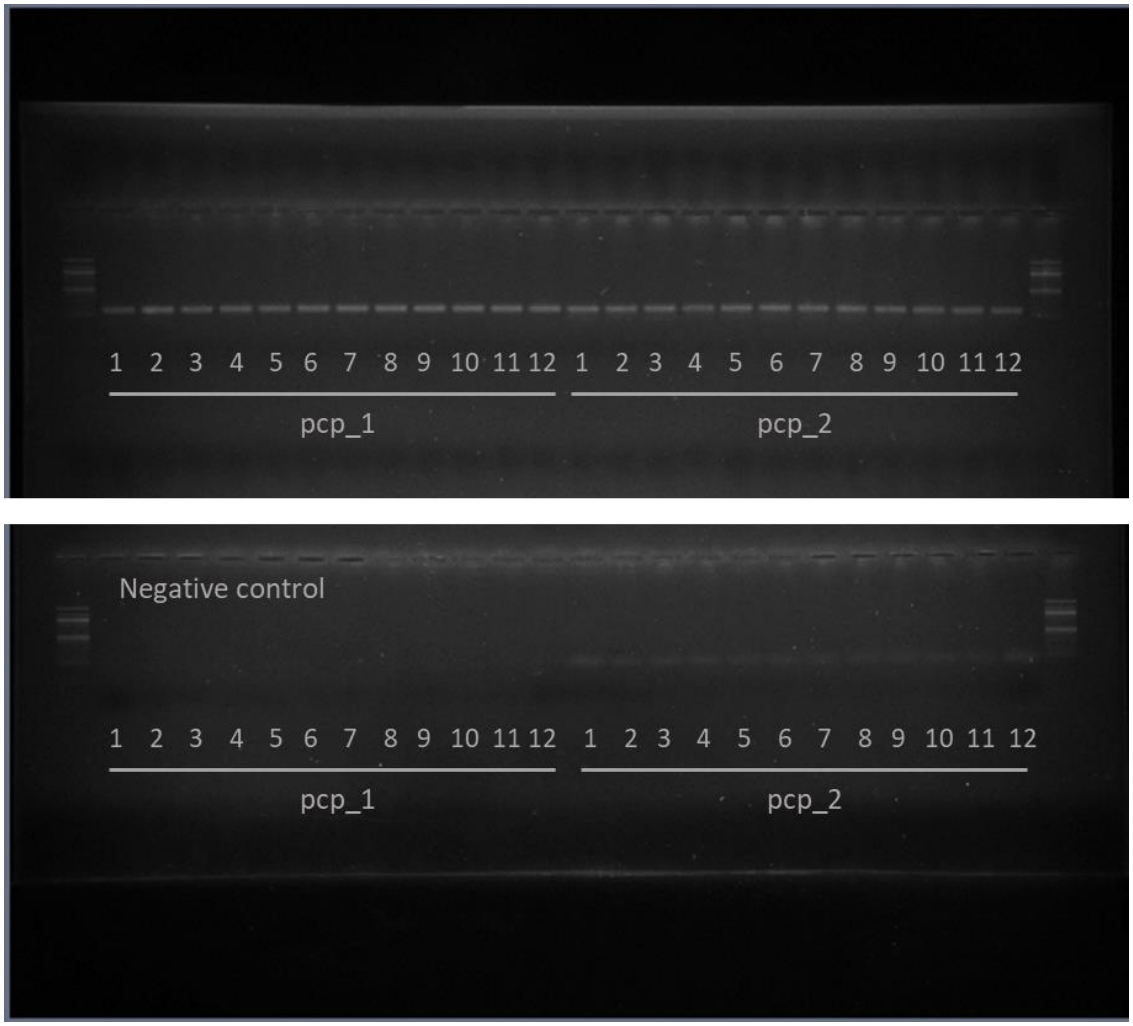

Figure E.3: Gradient PCR products and negative controls generated by pcp_1_F/R and pcp_2_F/R primers.

Figure E.4: Gradient PCR products and negative controls generated by tnpA_1_F/R and tnpA_2_F/R primers.

Appendix F: Effect of DNase treatment

Cq values before and after additional DNase treatment of T16 RNA eluates are listed in table F.1.

Table F.1: Effect of DNase treatment based on Cq values. The table shows an overview of difference in DNA concentrations in RNA eluates before and after DNase treatment based on Cq values generated with specific primers. The RNA eluates derive from T16, both from cells in exponential and stationary growth phase at 37 °C. There are triplicates of each condition.

	Cq values of RNA eluate triplicates before DNase treatment						**Cq values of RNA eluate triplicates after DNase treatment**					
	Exponential phase			**Stationary phase**			**Exponential phase**			**Stationary phase**		
	1	**2**	**3**	**1**	**2**	**3**	**1**	**2**	**3**	**1**	**2**	**3**
repFIB_1	23	25	24	25	25	24	36	35	34	32	32	32
repFIB_2	23	24	24	24	24	23	N/A	39	N/A	N/A	38	N/A
c1_1	23	24	24	24	24	23	39	39	38	39	37	38
c1_2	24	25	25	25	25	24	33	N/A	34	35	34	36
pcp_1	24	25	25	25	24	24	38	36	34	35	36	36
pcp_2	26	28	27	28	27	27	37	36	37	37	36	36
tnpA_1	23	24	24	24	24	24	35	35	36	34	35	35
tnpA_2	27	29	28	28	27	27	35	36	35	38	N/A	39

Appendix G: Effect of conditions on phage P1 - Primer pair 2.

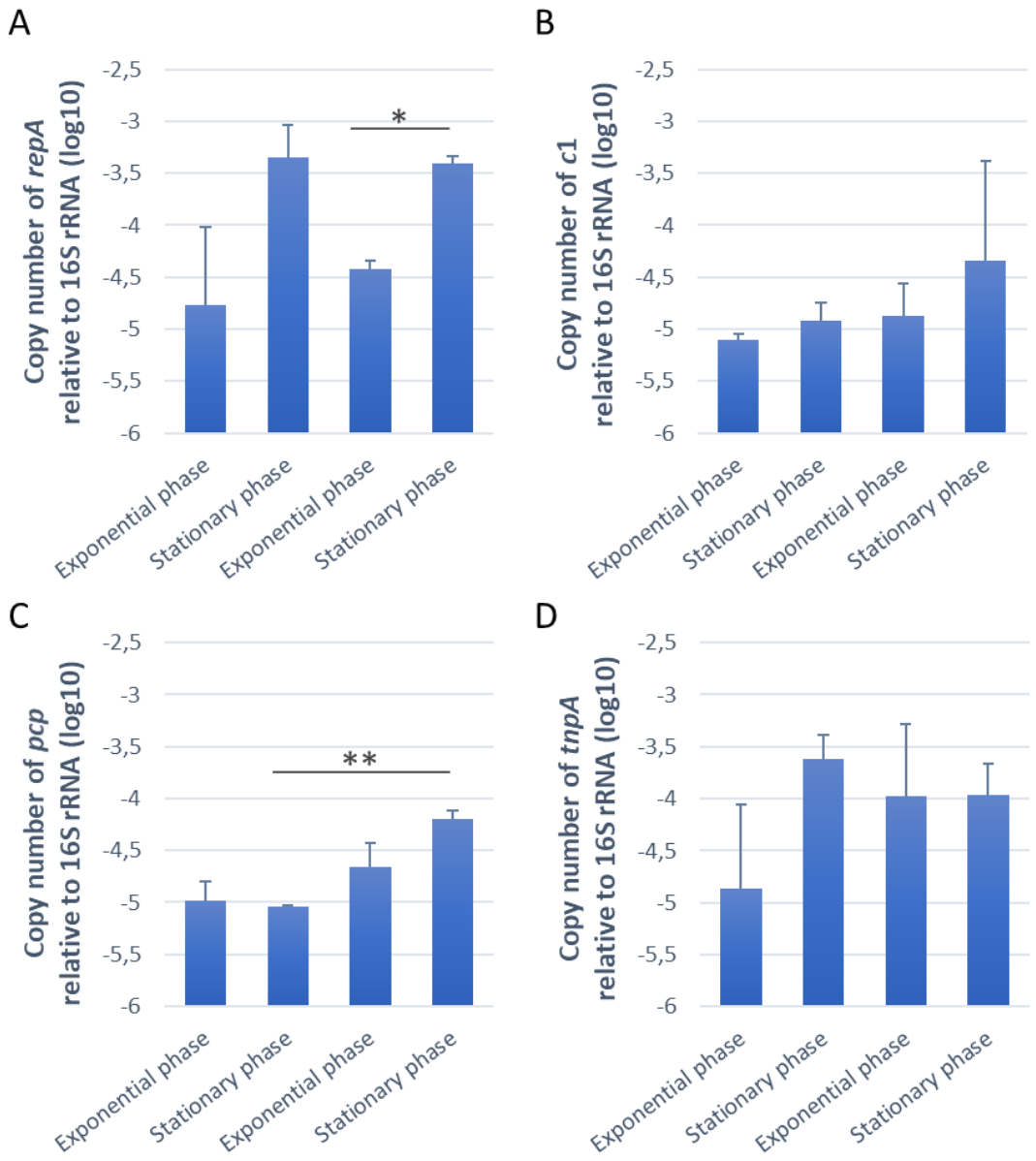

Figure G.1: Effect of growth phase and temperature on phage P1 transcription. Schematic diagrams of phage P1 transcription of P1 and Tn*21* genes in T16 during exponential and stationary bacterial growth phase, cultivated at both 37 ºC and 42 ºC. The effect is shown as copy number relative to 16S rRNA of (A) the *repA* replication protein A gene, (B) the *c*1 repressor gene, (C) the phage capsid protein (*pcp*) gene and (D) the *tnpA* transposase gene. The values are the mean of triplicates and are log transformed. The standard deviations of the values are indicated. Primer pair 2 is used. *p<0.05 and **p<0.01.

Appendix H: Effect of conditions on P1 copy number - Primer pair 2.

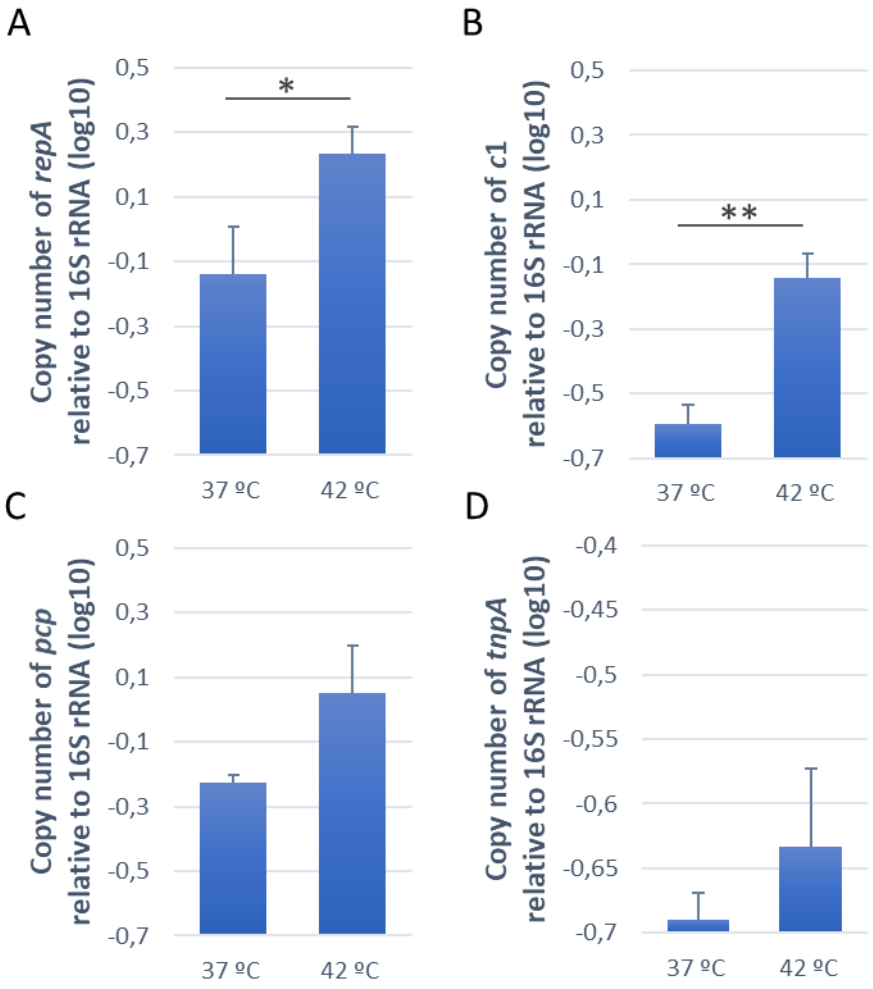

Figure H.1: Effect of cultivation temperature on phage P1 copy number. Schematic diagrams of copy number relative to 16S rRNA of phage P1 related genes in T16 at stationary growth phase at 37 ºC and 42 ºC. The genes shown are (A) *repA* replication protein A gene, (B) *c*1 repressor gene, (C) phage capsid protein (*pcp*) gene and (D) *tnpA* transposase gene. Notise that the axis in (D) deviates from the other diagrams. The values are log transformed means of triplicates, and the standard deviations are indicated. Primer pair 1 is used. *$p<0.05$ and *$p<0.01$.

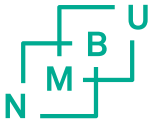

Norges miljø- og biovitenskapelige universitet
Noregs miljø- og biovitskapelege universitet
Norwegian University of Life Sciences

Postboks 5003
NO-1432 Ås
Norway